

Copyright © 1980, by the author(s).
All rights reserved.

Permission to make digital or hard copies of all or part of this work for personal or classroom use is granted without fee provided that copies are not made or distributed for profit or commercial advantage and that copies bear this notice and the full citation on the first page. To copy otherwise, to republish, to post on servers or to redistribute to lists, requires prior specific permission.

ARNOLD DIFFUSION IN HAMILTONIAN SYSTEMS

WITH THREE DEGREES OF FREEDOM

by

M. A. Lieberman

Memorandum No. UCB/ERL M79/83

1 February 1980

ELECTRONICS RESEARCH LABORATORY

College of Engineering
University of California, Berkeley
94720

ARNOLD DIFFUSION IN HAMILTONIAN SYSTEMS
WITH THREE DEGREES OF FREEDOM[†]

by

M.A. Lieberman*

Department of Physics

Imperial College of Science and Technology

London, U.K.

* Permanent address: Department of Electrical Engineering
and Computer Sciences, University of California, Berkeley,
Calif. 94720.

[†] Work supported by the Office of Naval Research Contract N00014-79-C-0674
and National Science Foundation Contract ENG 78-26372.

ABSTRACT

We review using a simple example the mechanism for a very general form of self-generated stochastic motion -- the Arnold diffusion -- which occurs in near-integrable Hamiltonian systems with three or more degrees of freedom. We consider the motion of a ball bouncing between a smooth wall located at $z=h$ and a periodically rippled wall located at $z=0$ with ripples along x and y . The ball's diffusive motion in phase space is calculated using a stochastic pump model, and compared with simulations for over 10^7 collisions of the ball with the rippled wall. The calculated diffusion rates are in good agreement with the simulation results. The results, which apply to the interaction of three nonlinear resonances in the system, are contrasted with recent calculations by others in the Nekhoroshev (many resonance) diffusion regime.

1. INTRODUCTION

We review, by means of a simple example, the mechanism for a very general form of self-generated stochastic motion -- the Arnold diffusion -- which occurs in near-integrable Hamiltonian systems¹ with three or more degrees of freedom. Without loss of generality, we consider autonomous systems, for which the Hamiltonian is explicitly independent of time. Non-autonomous systems in N degrees of freedom can be made autonomous in $N+1$ degrees of freedom by introducing an extended phase space¹. "Near integrable" Hamiltonians have the form $H = H_0 + \epsilon H_1$ with H_0 integrable, H not integrable, and the perturbation strength $\epsilon \ll 1$.

The generic behaviour of near-integrable systems with two degrees of freedom is now reasonably well known²⁻⁴. Such systems possess a finite fraction of trajectories which are the integrable trajectories of KAM theory, with the remaining fraction appearing to be stochastic. The integrable trajectories depend discontinuously on initial conditions. Stochastic and integrable trajectories are intimately co-mingled, with some stochastic trajectory lying arbitrarily close to every point in the four dimensional phase space, and in the two dimensional surface of section. The stochastic trajectories form in the neighbourhood of resonances of the motion between the two degrees of freedom. They appear as thin layers of stochasticity surrounding the separatrices of the motion associated with these resonances. The thickness of the layers increases with increasing perturbation strength. For weak perturbation, stochastic

layers associated with different resonances are isolated from each other by KAM surfaces. The motion is stable, either lying in a KAM surface, or within a thin stochastic layer which is bounded by nearby KAM surfaces. As the perturbation increases, the thickness of the layers expands, leading to resonance overlap, the destruction of the last KAM surface separating the layers. This signals the sudden appearance of strong stochasticity in the motion, in which the previously separated layers have merged, and the trajectory freely moves across the layers.

The nature of the motion in systems with three or more degrees of freedom is similar to the above in most respects. Stochastic and integrable (KAM) trajectories are intimately comingled in the $2N$ dimensional phase space. Stochastic layers form near the separatrices associated with resonances of the motion among the degrees of freedom. For strong perturbation, resonance overlap leads to motion across the layers and the presence of strong stochasticity. In the limit of weak perturbation, however, resonance overlap does not occur. A new physical behaviour⁵ of the motion then makes its appearance: stochastic motion along the resonance layers -- the so-called weak stochasticity or Arnold diffusion. This motion is the consequence of a fundamental geometric fact: For $N > 3$, the $2N-1$ dimensional resonance layers are not isolated from each other by the N dimensional KAM surfaces. The situation is analogous to that illustrated in Fig.1, where "KAM lines" isolate regions of a plane, but do not separate a three dimensional volume into distinct regions. As a result, all stochastic layers are connected

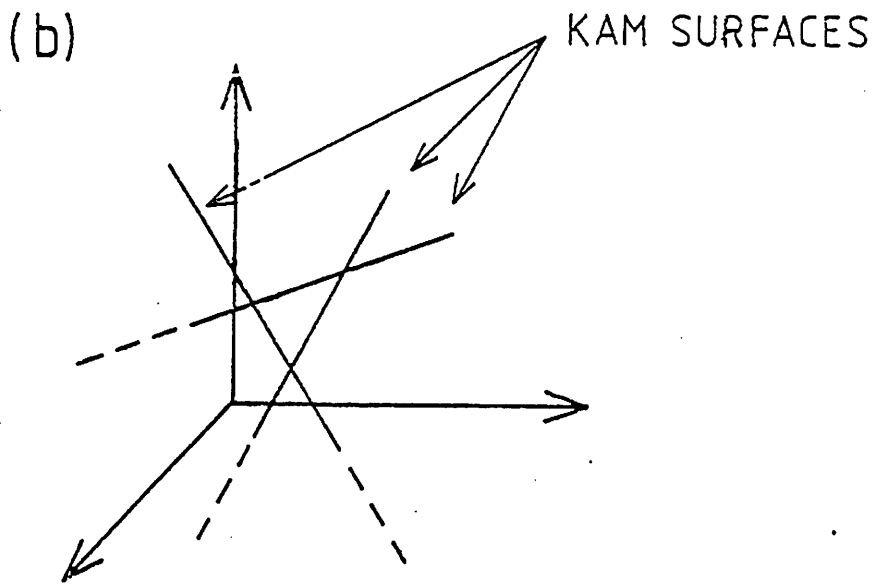
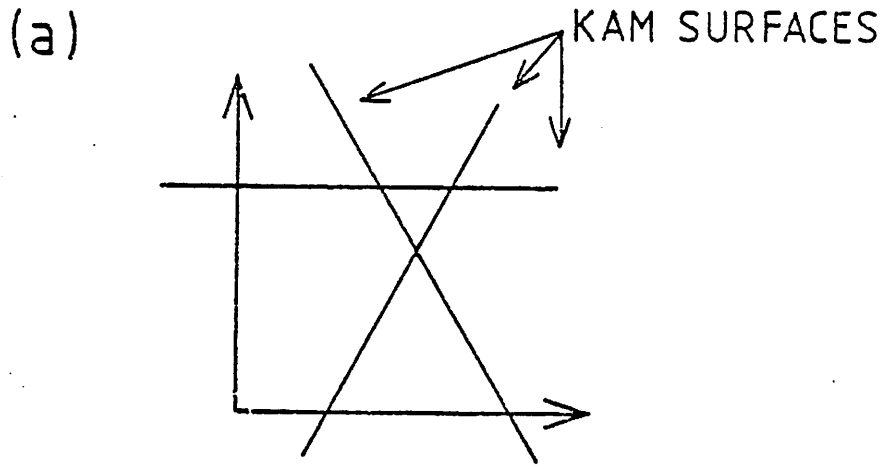


Fig.1 Isolation of regions by KAM surfaces (lines). In (a), the plane is divided by lines into a set of closed areas; in (b), the volume is not divided by lines into a set of closed volumes.

into single complex network -- the Arnold web. The web consists of an intricate system of "freeways, streets, sidewalks, and cracks" that permeates the entire phase space, intersecting or lying infinitesimally close to every point. For an initial condition within the web, the subsequent stochastic motion will eventually intersect every finite region of the phase space, even the predominantly stable regions where the fraction of stochastic initial conditions is small, and even in the limit as the perturbation strength $\epsilon \rightarrow 0$. This motion is the Arnold diffusion.

The merging of stochastic trajectories into a single web was proved by Arnold⁵ for a specific nonlinear Hamiltonian. A general proof of the existence of a single web has not been given, but many computational examples are known. From a practical point of view, there are two major questions concerning Arnold diffusion in a particular system:

- (1) what is the relative measure of stochastic trajectories in the phase space region of interest? and
- (2) for a given initial condition, how fast will the system diffuse along the thin threads of the Arnold web.

The extent of the web in phase space can be estimated by means of resonance overlap conditions⁴. Overlap of resonances gives rise to a resonance layer thickness, with stochastic motion occurring across the layer as in systems with two degrees of freedom. The new feature of Arnold diffusion is the presence of stochastic motion along the resonance layer. produced as a result of the coupling of at least three resonances, coupling at least three degrees of freedom.

We illustrate the motion along a resonance layer in Fig.2. A projection of the motion onto the J_1 - θ_1 action-angle plane is shown, illustrating a resonance with the stochastic layer surrounding its separatrix. At right angles to this plane the action J_2 associated with a second degree of freedom is shown. The fast diffusive motion across the layer, and the slow Arnold diffusion along the layer are illustrated. Since J_1 always lies within the thin resonant layer, a large change in J_2 is possible only if a third degree of freedom is present. The action in this third degree of freedom must also change, maintaining the energy constant as diffusion along the layer proceeds.

Calculation of the diffusion rate along a layer has been given by Chirikov⁴ and Tennyson *et al*⁶ for the important case of three resonances, and will be considered here in some detail. For coupling among many resonances, a rigorous upper bound on the diffusion rate has been obtained by Nekhoroshev⁷, but this bound generally overestimates the rate by many orders of magnitude. A statistical treatment of the diffusion regime in which many resonances are important is under development^{4,8,9}, and some recent results will be described. Extensive numerical simulations of Arnold diffusion have been carried out^{4,6,9-11} and are summarized in the review article by Chirikov⁴.

II BILLIARDS PROBLEM

Simple examples of coupled systems can be constructed to illustrate Arnold diffusion. One such system, which we

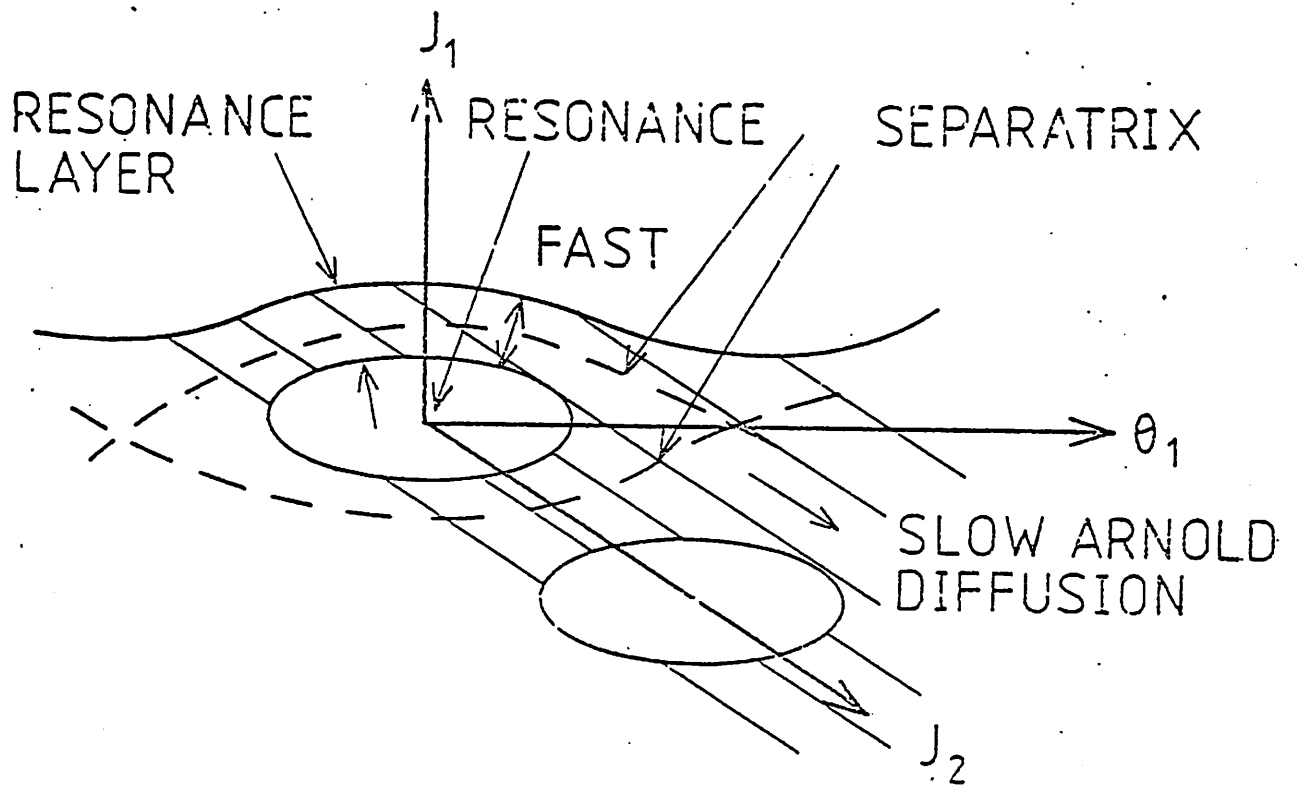


Fig.2 An illustration of Arnold diffusion. The resonance is at the origin, with the separatrix surrounding it. Stochastic motion across the layer, and the slow Arnold diffusion along the layer, are shown.

consider extensively here, is that of a ball bouncing back and forth between a smooth wall at $z=h$ and a fixed wall at $z=0$ which is rippled in two dimensions, x and y . The surface of section is given in terms of the ball positions in the x_n and y_n directions and the trajectory angles $\alpha_n = \tan^{-1} v_x/v_z$ and $\beta_n = \tan^{-1} v_y/v_z$, just before the n th collision with the rippled wall. The ball motion is shown schematically in Fig.3, and the definitions of the variables in the x, z plane shown in Fig.4. Assuming that the ripple is small, the rippled wall may be replaced by a flat wall at $z=0$ whose normal vector is a function of x and y , analogous to the idea of a Fresnel mirror. The simplified difference equations exhibit the general features of the exact equations and may be written in explicit form

$$\alpha_{n+1} = \alpha_n - 2 a_x k_x \sin k_x x + \mu k_x \gamma_c \quad (1)$$

$$x_{n+1} = x_n + 2 h \tan \alpha_{n+1} \quad (2)$$

$$\beta_{n+1} = \beta_n - 2 a_y k_y \sin k_y y + \mu k_y \gamma_c \quad (3)$$

$$y_{n+1} = y_n + 2 h \tan \beta_{n+1} \quad (4)$$

where $\gamma_c = \sin (k_x x + k_y y)$, a_x and a_y are the amplitudes of the ripple in the x and y directions respectively, and μ is the amplitude of the diagonal ripple and represents the coupling between the x and y motions. A similar set of equations has been studied numerically by Froeschle¹⁰.

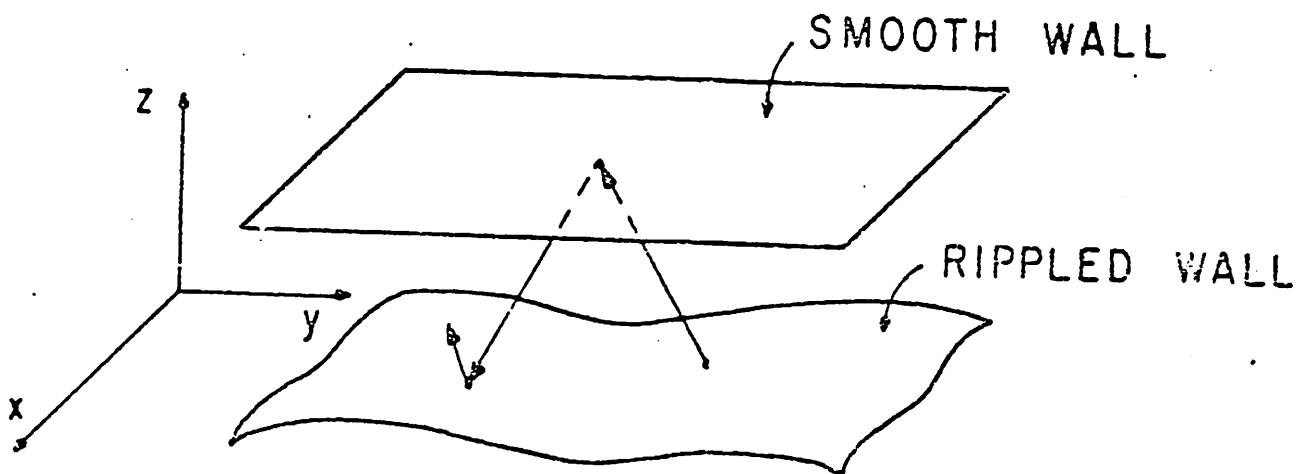


Fig.3 The three dimensional billiards problem. A point particle bounces back and forth between a smooth and a periodically rippled wall.

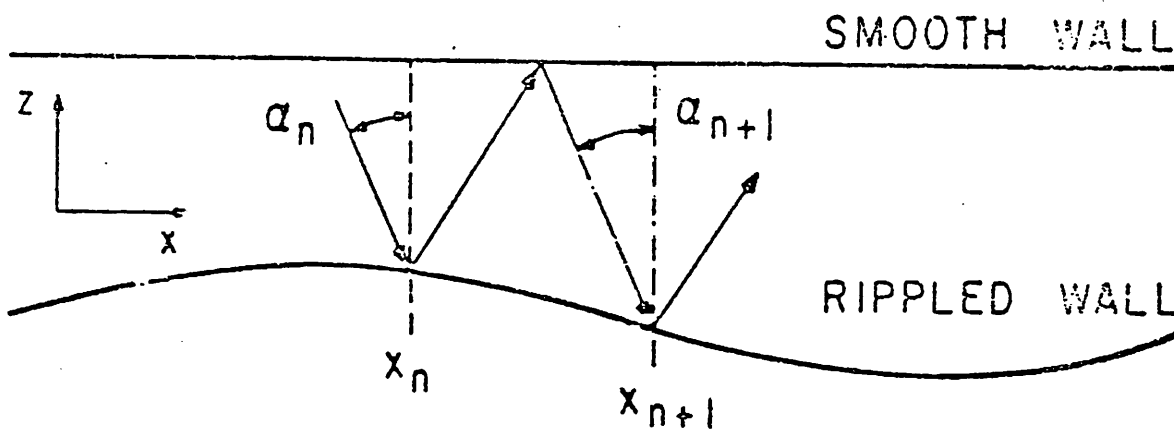


FIGURE 10.

The definitions of α_n and x_n

Fig.4 Motion in two degrees of freedom, illustrating the definition of the angle of incidence (action) α_n , and the bounce position x_n just before the n^{th} collision with the rippled wall.

If $\mu=0$, the system breaks into two uncoupled parts describing motion in x-z and y-z separately. Fig.5 shows the motion in the α -x surface of section for the uncoupled case. A number of different trajectories are shown, each with different initial conditions. Each particle was run for 1000 iterations. The plot displays the usual features of a system with two degrees of freedom: (1) stable (KAM) trajectories (2) resonance islands and (3) stochastic trajectories. The islands are examples of "higher order" integrable (KAM) trajectories. There are two major stochastic trajectories visible in Fig.5. The thick stochastic layers for $|\alpha| \gtrsim 0.6\pi/2$ are regions of strong stochasticity produced by all overlapping resonances with one bounce period in z equal to k periods along x, for $k \geq 1$. The thin stochastic layer has formed in the neighbourhood of the separatrix associated with the central (k=0) resonance.

III STOCHASTIC PUMP DIFFUSION CALCULATION

We examine three of the Arnold diffusion processes that characterize the system, (1)-(4). The first describes the diffusion of α along the thick stochastic layer of the β -y motion. The quantity α experiences diffusive fluctuations that result from the small coupling to the random y motion. The second process is similar to the first, except that α now diffuses along the thin separatrix layer of the β -y motion. The third process occurs near a coupling resonance between the x and y motions, chosen so that the periods of oscillation

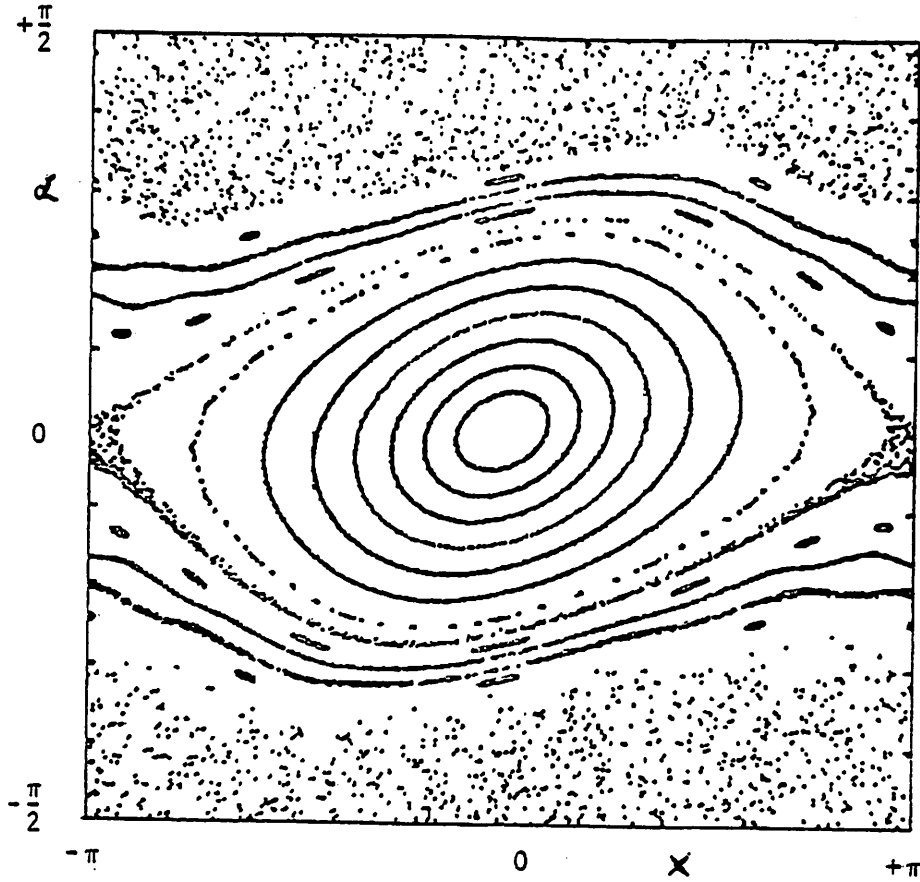


Fig.5 Motion in the α - x surface of section for the uncoupled billiards problem. The parameters are $\mu=0$, with $\lambda_x:h:a_x$ as 100:10:2; $\lambda_x = 2\pi/k_x$. Fifteen particles are started at $x=0$ for various α 's and allowed to run for 1000 iterations each.

around the central resonance for the x and y motions are the same. Thick layer diffusion tends to be much faster than thin layer diffusion due to the greater randomness of the y motion in the former case. The coupling resonance diffusion is very slow.

In order to calculate the diffusion rates, we adopt a simple model of the diffusion process. For both the "thin" and "thick" layer processes, we assume that the y motion is confined to the stochastic layer. It then acts as a stochastic pump, transporting energy back and forth between the x and z motions. Its own energy may not change except for the small fluctuations necessary to effect the pumping action. (Note that this is not strictly true. It is possible for the y-motion to leave the main stochastic layer along a thin "alleyway", but this turns out to be very unlikely). For coupling resonance diffusion, a transformation to new generalized coordinates must be made to explicitly exhibit the separatrix and its associated stochastic layer. The calculation then proceeds as in thin layer diffusion.

The first step in the calculation is to find a Hamiltonian that will generate the surface of section mappings, (1) - (4). In deference to our original model in Fig.3 we choose a "kicked" Hamiltonian

$$H(\alpha, x, \beta, y, n) = 2h \ln \sec \alpha + 2h \ln \sec \beta - 2\delta_1(n)C(x, y) \quad (5)$$

where

$$C(x, y) = a_x \cos k_x x + a_y \cos k_y y - \frac{1}{2} \mu \cos (k_x x + k_y y) \quad (6)$$

and

$$\begin{aligned}\delta_1(n) &\equiv \sum_{m=-\infty}^{+\infty} \delta(n-m) \\ &= 1 + 2 \sum_{q=1}^{\infty} \cos(2\pi nq).\end{aligned}\tag{7}$$

Equations (1) - (4) may be derived from (5) by a simple integration of Hamilton's equations. Note that H in Eq.(5) is a nonautonomous Hamiltonian in two degrees of freedom. It is related to the net energy in the x and y motion, and is not conserved.

IV THICK LAYER DIFFUSION

The initial conditions appropriate to thick layer diffusion have β and y within the thick stochastic layer, with α and x chosen to yield small amplitude libration near the central resonance. In the absence of coupling $\mu=0$, the motion in the α - x plane is confined to a smooth closed curve, like those seen close to the center of Fig.5. For a finite coupling, α and x diffuse slowly due to the small randomizing influence of the stochastic β - y motion. The diffusion is shown in Fig.6 for 2,000, 10,000, and 30,000 iterations. The motion eventually explores all of the α - x plane. The corresponding motion in the β - y plane is restricted to the thick stochastic layer, at least until the α - x motion reaches its own thick layer.

For the initial conditions appropriate to thick layer diffusion, we decompose $H = H_x + H_y$, with

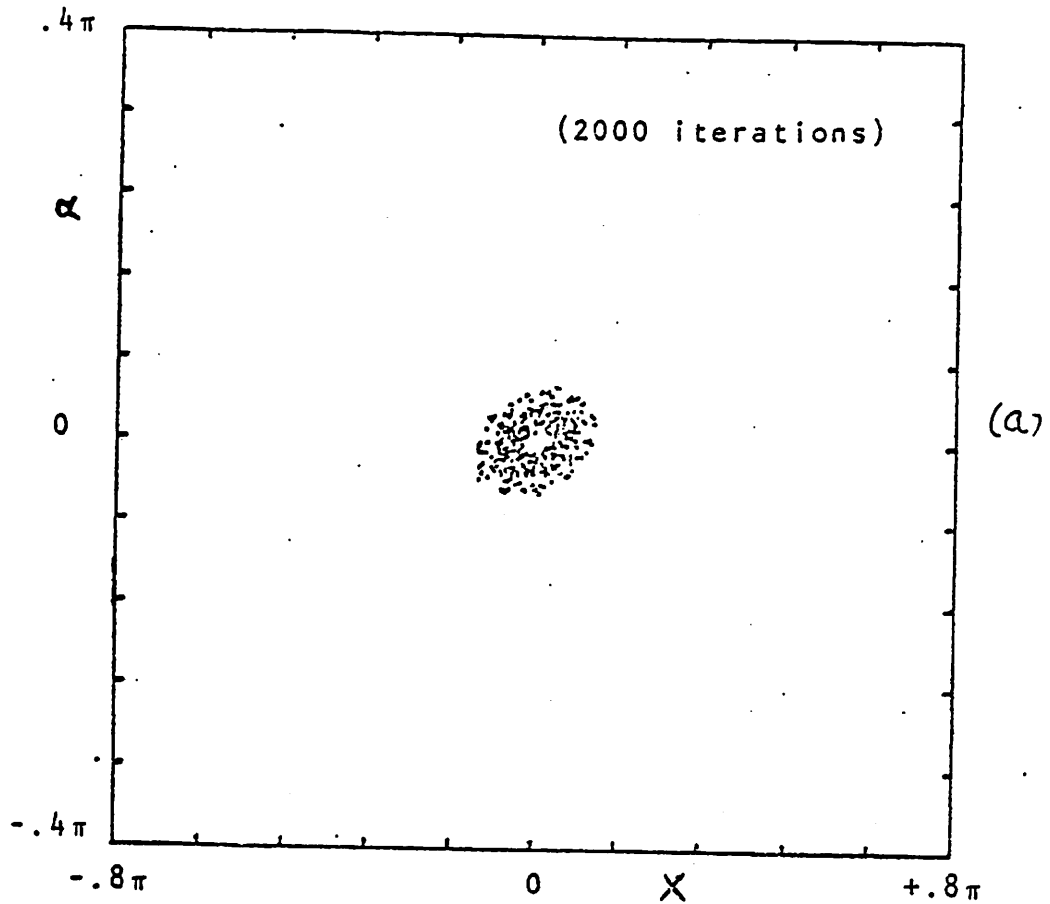
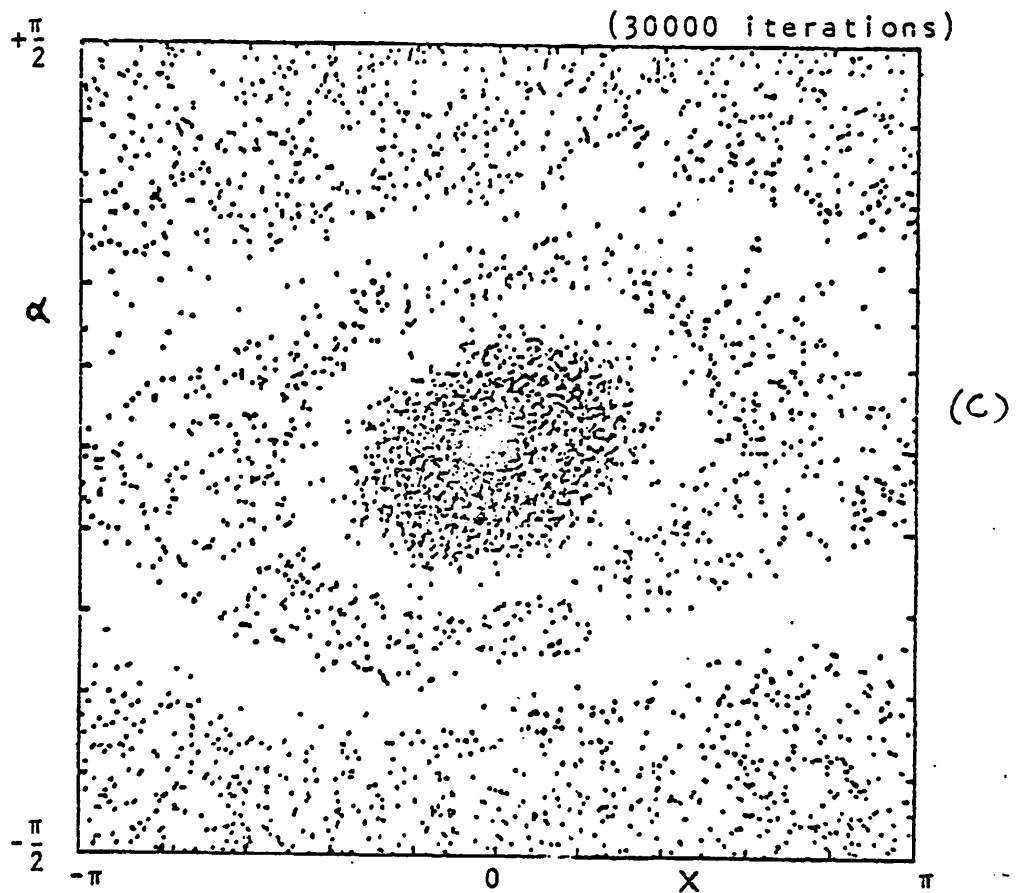
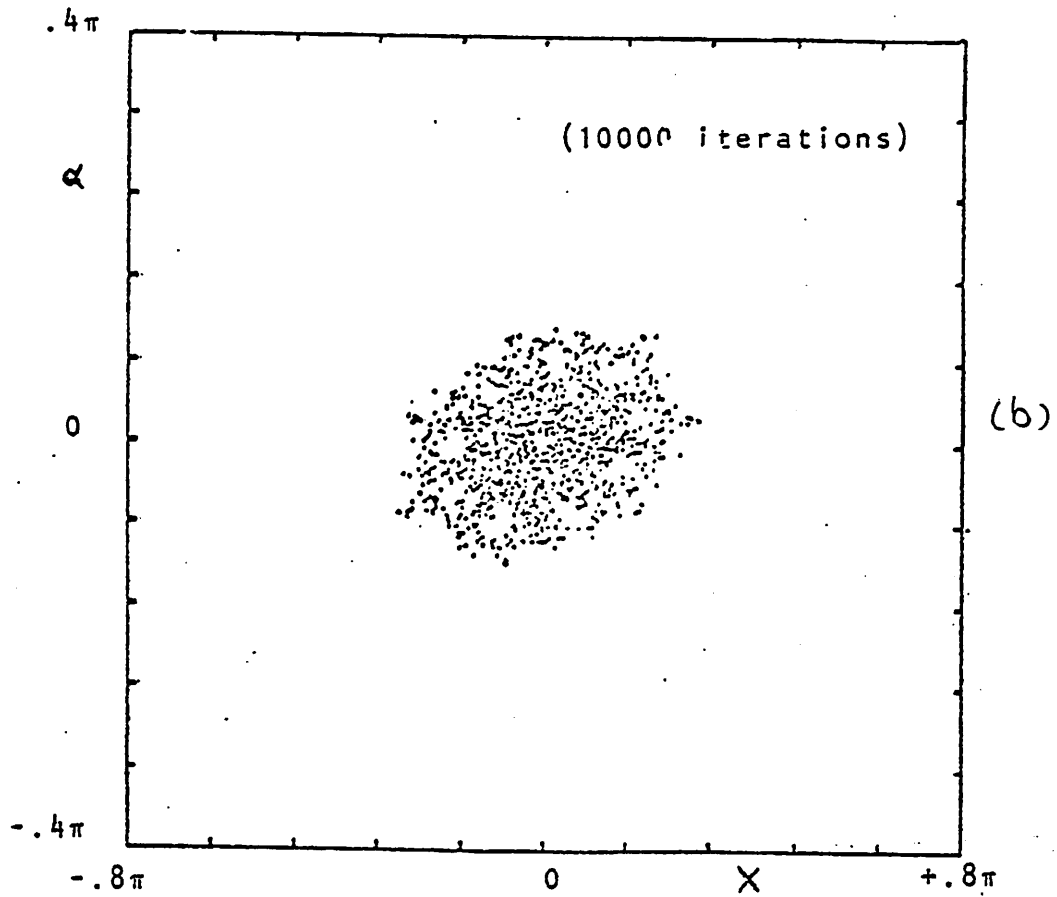
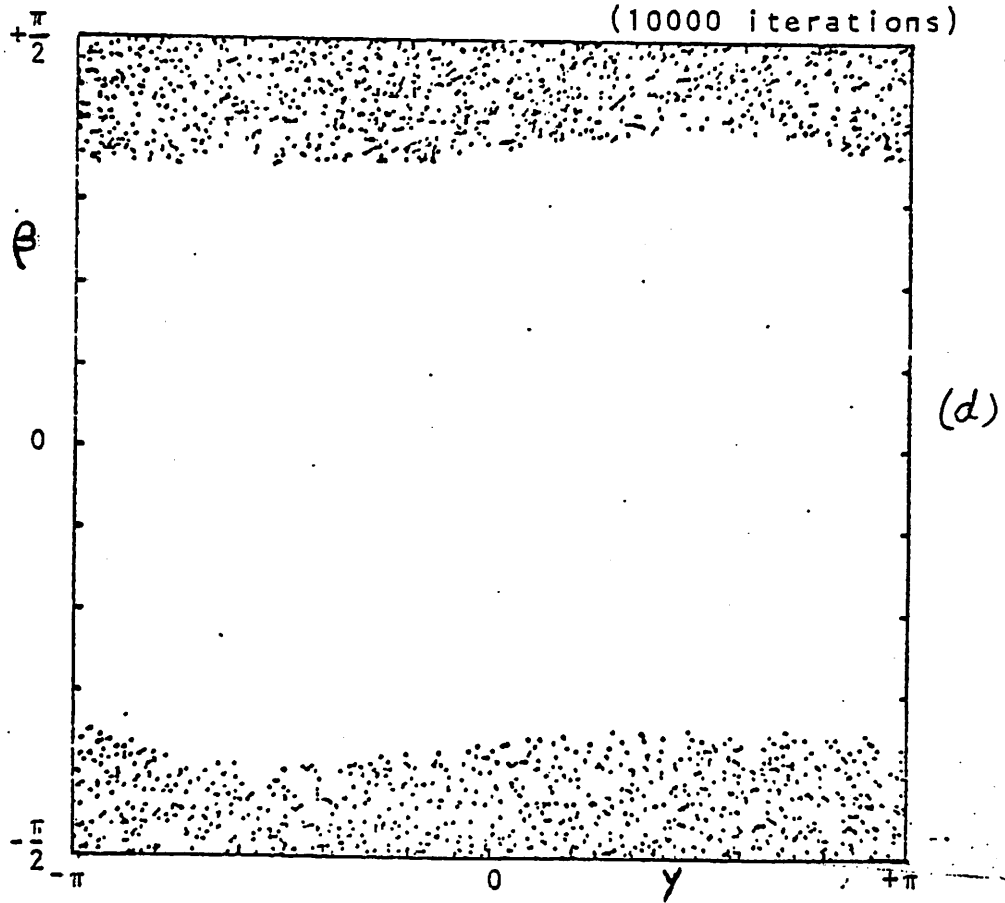


Fig.6 Thick layer diffusion for the coupled billiards problem. Initial conditions are close to the central resonance in the α - x space and within the thick stochastic layer (near $|\beta| = \pi/2$) of the β - y space. Parameters are $\mu/h = .008$ with $\lambda_x:h:a_x$ and $\lambda_y:h:a_y$ as 100:10:2.





$$H_y = 2 h \ln \sec \beta - 2 \delta_1(n) a_y \cos \phi \quad (8)$$

and

$$H_x = h \alpha^2 - 2 a_x \cos \theta + \mu \cos [\theta + \phi(n)] , \quad (9)$$

where we have written $\theta = k_x x$, $\phi = k_y y$, set $\ln \sec \alpha \approx \alpha^2/2$ since $\alpha^2 \ll 1$, and where ϕ in (9) is now considered to be an explicit function of n . This decomposition is a whopping big assumption, neglecting the coupling term in (8) and setting $\delta_1 \equiv 1$ in (9). By this means, we obtain two non-autonomous Hamiltonians, each in one degree of freedom. We solve first for the β - ϕ motion, "the stochastic pump", and, substituting this motion into (9), find the α - θ motion, whose diffusive component is the Arnold diffusion.

The motion for $\phi(n)$ generated by (8) is the well-known strong stochasticity in the thick layer. To a good approximation, ϕ makes a sudden random jump to a new phase whenever n is an integer¹². The Arnold diffusion coefficient D_1 for thick layer diffusion is calculated using this assumption as follows:

The evolution of H_x , from (9), is:

$$\frac{dH_x}{dn} = \frac{\partial H_x}{\partial n} = \frac{d}{dn} [\mu \cos(\theta + \phi)] - \mu \frac{d\theta}{dn} \sin [\theta + \phi(n)] . \quad (10)$$

The first term contributes only a small oscillation with no net change over long periods of time. For slow, small amplitude libration in the α - x plane, we have:

$$\theta = \theta_0 \cos(\omega_x n + \chi_0) , \quad (11)$$

where

$$\omega_x = 2\pi/T_x = 2 k_x (a_x h)^{1/2}$$

Using this, we integrate the second term in (10) over the "time" interval from m to $m+1$.

$$\Delta H_x = \int_m^{m+1} dn \mu \theta_o \omega_x \sin[\omega_x n + \chi_o] \sin[\theta + \phi(n)]. \quad (12)$$

For $\omega_x \ll 1$, this is

$$\Delta H_x = \mu \theta_o \omega_x \sin[\omega_x m + \chi_o] \sin[\theta + \phi(m)]. \quad (13)$$

We square this and average over both χ_o and ϕ to get

$$\langle \Delta H_x^2 \rangle = \frac{1}{4} \mu^2 \theta_o^2 \omega_x^2 \quad (14)$$

where we have used the assumption that ϕ is randomized at m -integer. The thick layer diffusion rate is then:

$$D_1 = \frac{1}{2} \langle \Delta H_x^2 \rangle = \frac{1}{8} \mu^2 \theta_o^2 \omega_x^2 \quad (15)$$

The parameters μ and ω_x will remain fairly constant as H_x diffuses. The quantity θ_o , however, increases with H_x , resulting in an increase in the diffusion rate as the x oscillations grow.

In Fig.7, the theoretical value of D_1 is compared with measurements obtained from the direct iteration of the difference equations. For each experiment, 100 particles

Fig.7 Thick layer diffusion. Comparison of the theoretical diffusion with the results of simulation experiments. In (a), the dispersion is plotted vs the coupling amplitude μ . In (b) the dispersion is plotted vs the libration period T_x . In (c), the dispersion vs the number of iterations n is shown. Parameters (except for those varied) are $\mu/h = .0002$; $n = 500$; $\lambda_x:h:a_x$ as 10:10:1; and $\lambda_y:h:a_y$ as 100:10:1.7. The statistical spread of the 100 particles is within the height of the triangles.

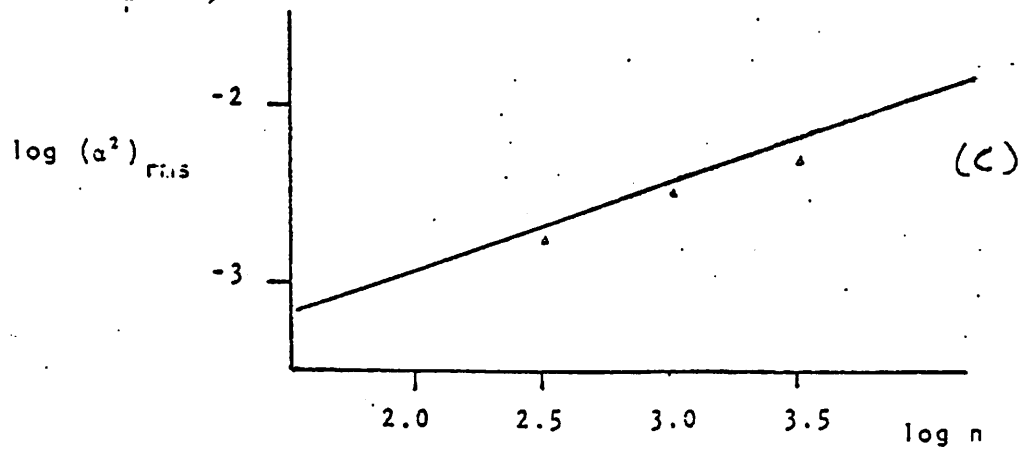
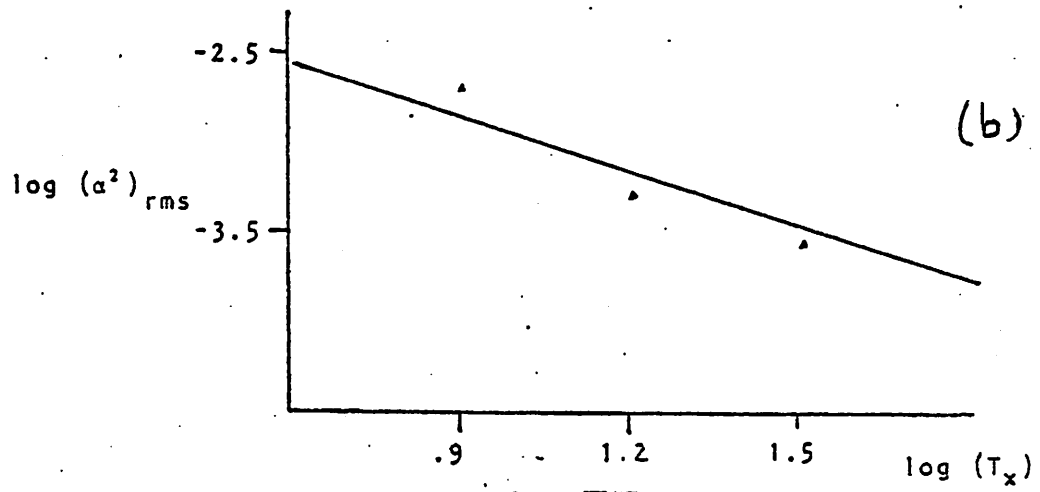
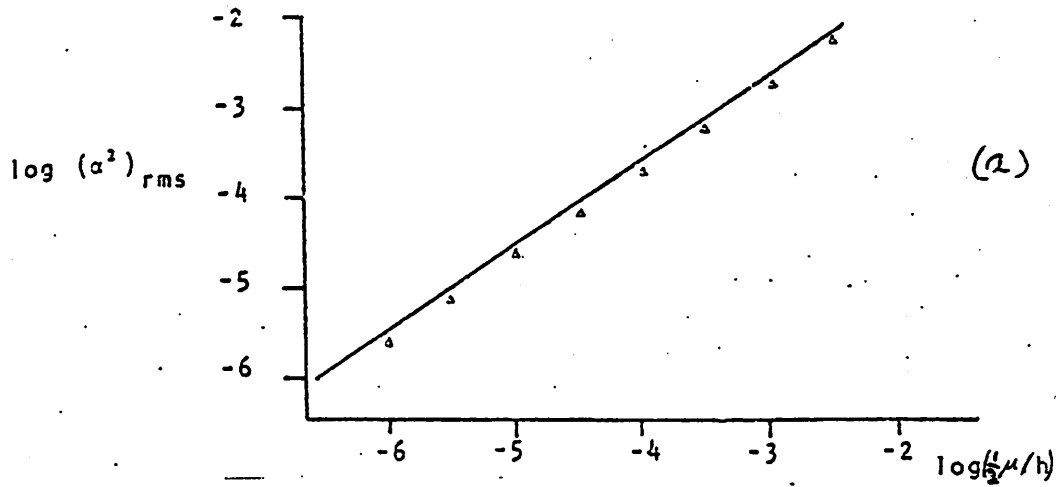
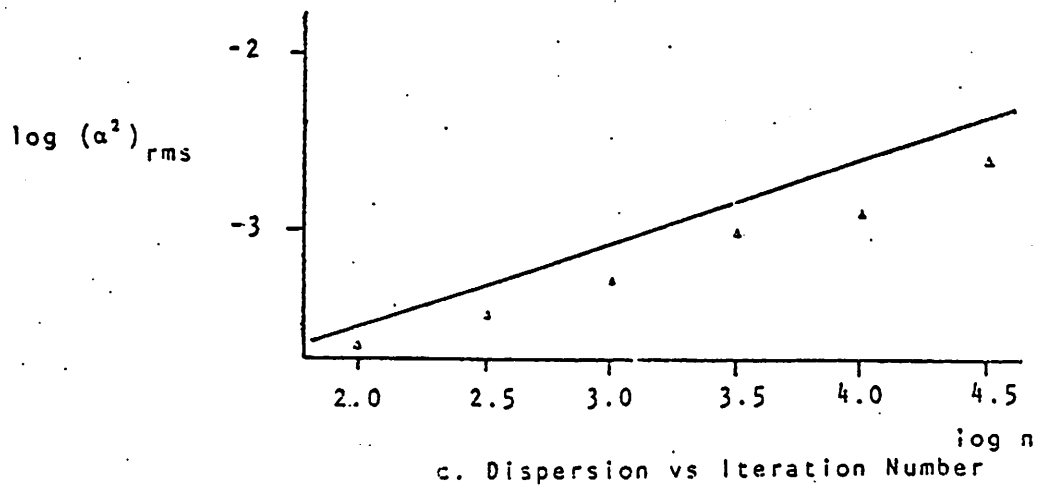
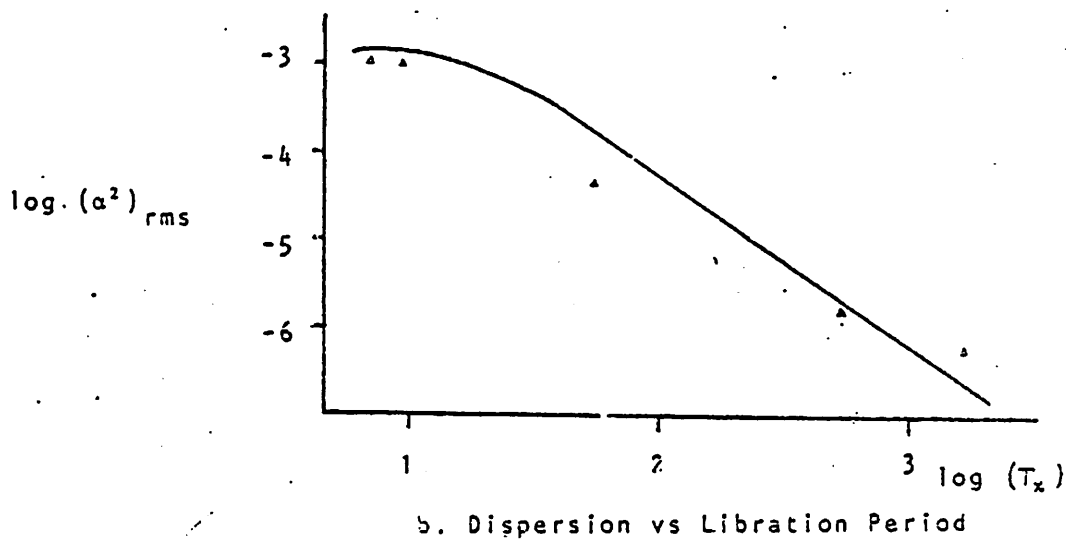
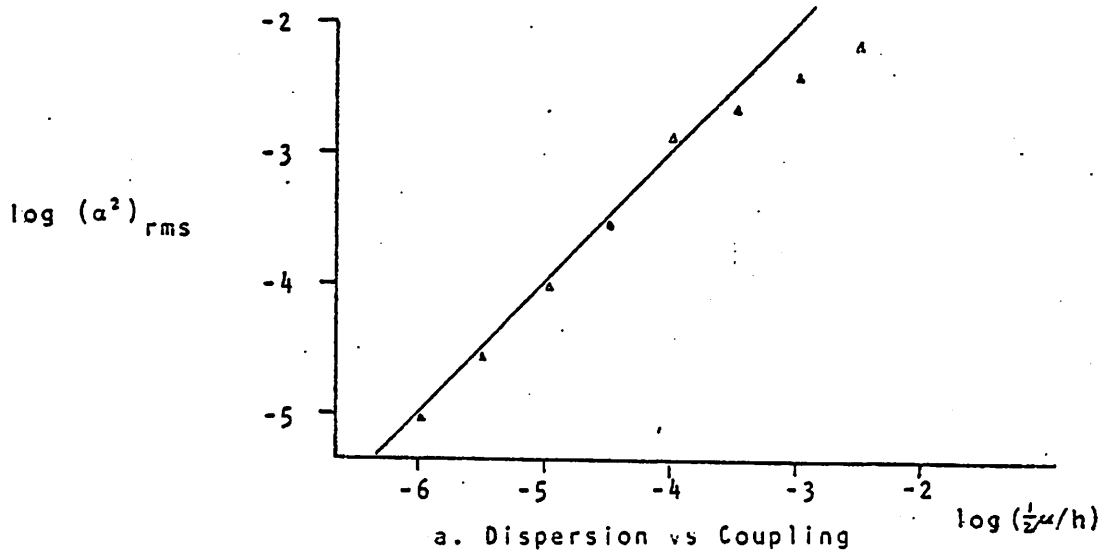


Fig.11 Thin layer diffusion. Comparison of the theoretical diffusion with the results of simulation experiments. The three graphs show the variation with μ , T_x and n . Parameters (except for those varied) are $\mu/h = .0002$; $n = 2000$; $\lambda_x:h:a_x$ as 100:10:1; and $\lambda_y:h:a_y$ as 100:10:1.8. The statistical spread of the 100 particles is within the height of the triangles.



were started with identical initial conditions on a libration curve of the α -x plane, and with random initial conditions in the thick stochastic layer of the β -y plane. The motion was followed for 500 collisions, and the RMS value of the energy $h(\alpha^2)_{\text{RMS}}$ was calculated and compared with the theory.

Figure 7a shows the variation with coupling strength μ , Fig. 7b the variation with period T_x , and Fig. 7c the variation with the number of iterations n . The solid lines show the theoretical predictions and the triangles the experimental measurements. Each triangle represents the average of four separate runs. The theoretical predictions, although consistently a little high, are quite good. The discrepancy probably reflects an expected small deviation from true random phase.

V. THIN LAYER DIFFUSION

We turn now to the thin layer diffusion. Although the initial conditions remain close to the central resonance of the α -x space, they are now chosen inside the thin stochastic layer surrounding the separatrix of the β -y space. The diffusion of the α -x motion is again caused by the small coupling to the stochastic y motion, but since thin layer trajectories are considerably less "random" than thick layer trajectories, the diffusion is significantly weaker.

An example of thin layer diffusion is shown in Fig. 8 where both the y and x motions are displayed on the same plot. The y motion is confined to its separatrix until the x motion reaches its own separatrix. The successive stages of the

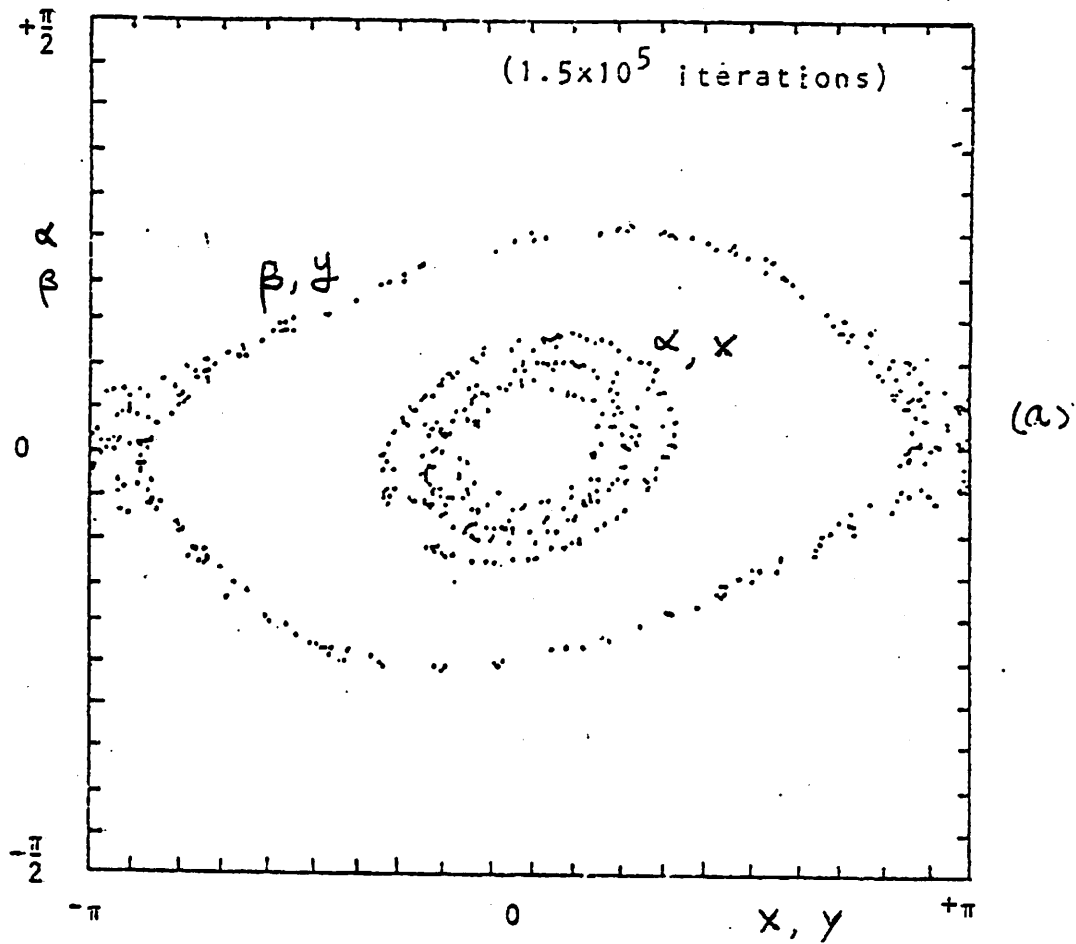
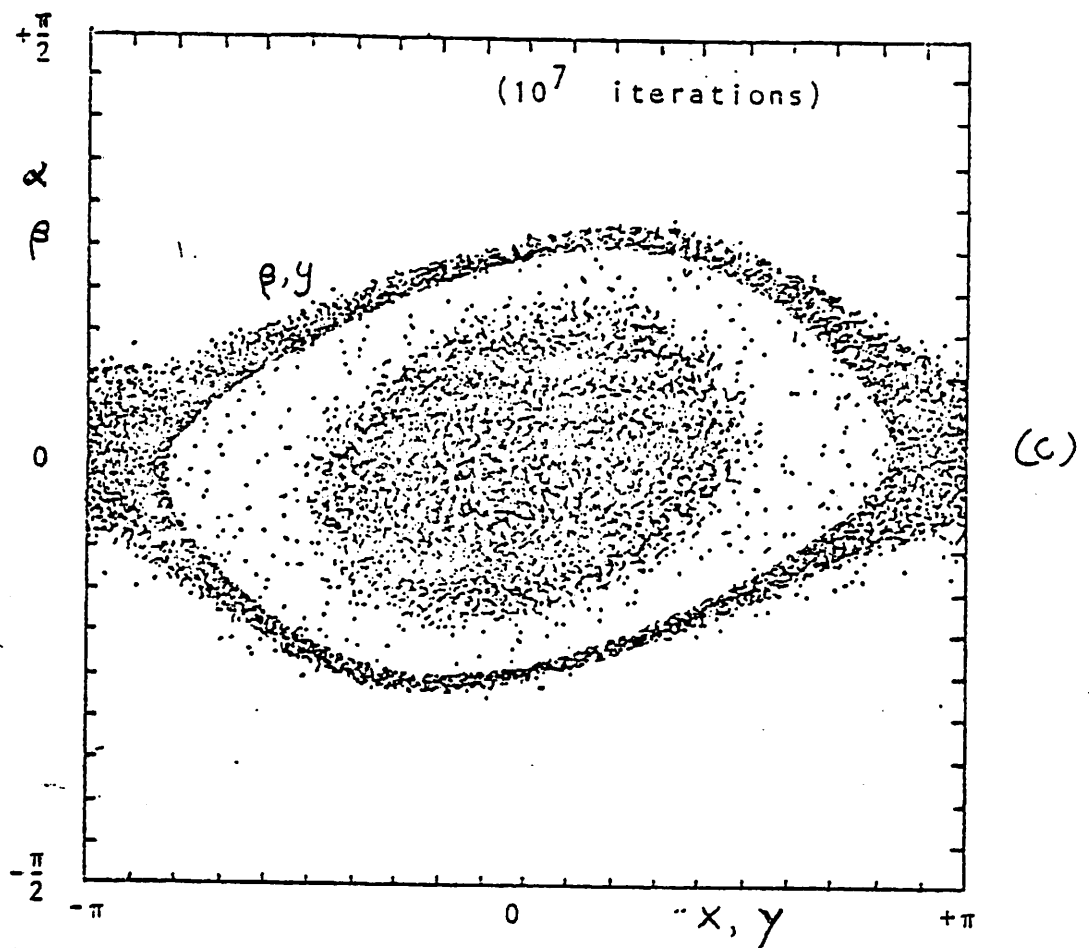
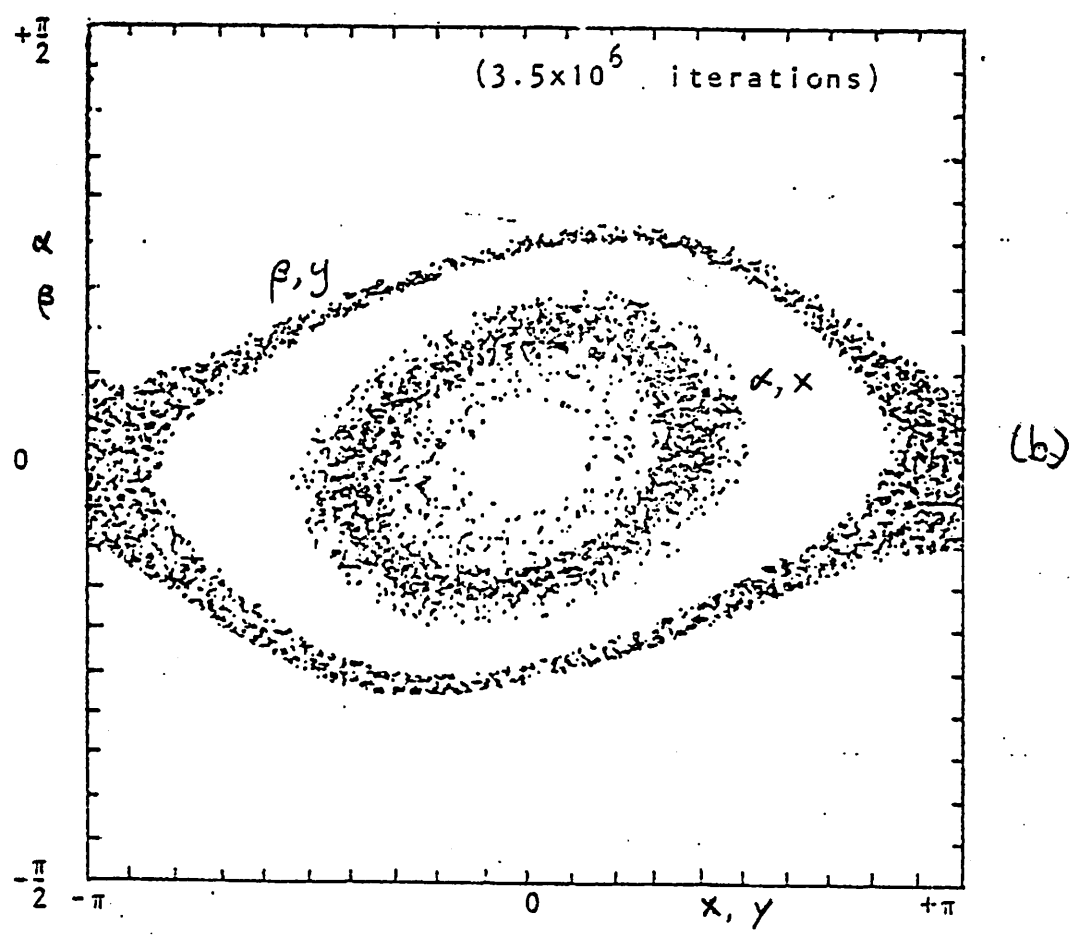


Fig.8 Thin layer diffusion. Initial conditions are close to the central resonance in the α - x space and within the separatrix stochastic layer in the β - y space. Parameters are the same as Fig.6. For convenience, both the α - x and β - y surface of sections are superimposed on the same figure.



diffusion of the α -x motion are shown in Fig.8a, b and c respectively.

To calculate the Arnold diffusion rate, we again decompose the Hamiltonian (5) into (8) and (9), where now, in (8), only the $q=0$ and $q=1$ terms in $\delta_1(n)$ need be kept. We also put $\ln \sec \beta \approx \beta^2/2$ for the separatrix motion, yielding, in place of (8),

$$H_y = h\beta^2 - 2a_y \cos \phi - 4a_y \cos 2\pi n \cos \phi. \quad (16)$$

In (16), the first two terms exhibit the separatrix associated with the central β -y resonance, and the third term generates the thin stochastic layer surrounding the separatrix. The procedure, as before, is to first solve (16), substitute the solution for $\phi(n)$ into (9), and then find the energy change ΔH_x as ϕ swings from $\phi = -\pi$ to $\phi = +\pi$. Starting with (10) and again neglecting the first term we have

$$\frac{dH_x}{dn} = -\mu \frac{d\theta}{dn} \sin [\theta + \phi(n)]. \quad (17)$$

As before, $\theta(n)$ corresponds approximately to small liberations, given by (11). But instead of randomizing $\phi(n)$ with each bounce, we now assume that it evolves very much like the phase on a pendulum separatrix

$$\phi(n) = 4 \tan^{-1} (e^{\omega_y n}) - \pi, \quad (18)$$

where ω_x and ω_y are the frequencies of small oscillations about the central fixed points of the α -x and β -y spaces, respectively:

$$\omega_x = 2k_x \sqrt{a_x \hbar} \quad , \quad \omega_y = 2k_y \sqrt{a_y \hbar}$$

A sketch of the separatrix phase motion and its derivative, the frequency, is given in Fig.9. The maximum frequency is $2\omega_y$ and occurs at the midpoint of the separatrix trajectory $n=0$. Defining:

$$s \equiv \omega_y n \quad , \quad r \equiv \omega_x / \omega_y \quad , \quad x_0 = rs_0 + \pi/2$$

then

$$\Delta H_x = \mu \theta_0 r \int_{-\infty}^{+\infty} ds I(s) \quad (19)$$

where

$$I = \cos [r(s+s_0)] \sin \{ \theta_0 \sin [r(s+s_0)] + \phi \} \quad (20)$$

Using $\theta_0 \ll 1$

$$I = \cos [r(s+s_0)] \sin \phi. \quad (21)$$

Only the symmetric part contributes to the integral.

$$I_{\text{sym}} = \frac{1}{2} \sin (rs_0) [\cos (\phi + rs) - \cos (\phi - rs)]. \quad (22)$$

The integrals in (19), now of the form:

$$A'_m = \lim_{s_1 \rightarrow \infty} \int_0^{s_1} 2 \cos \left[\frac{m}{2} \phi(s) \pm rs \right], \quad (23)$$

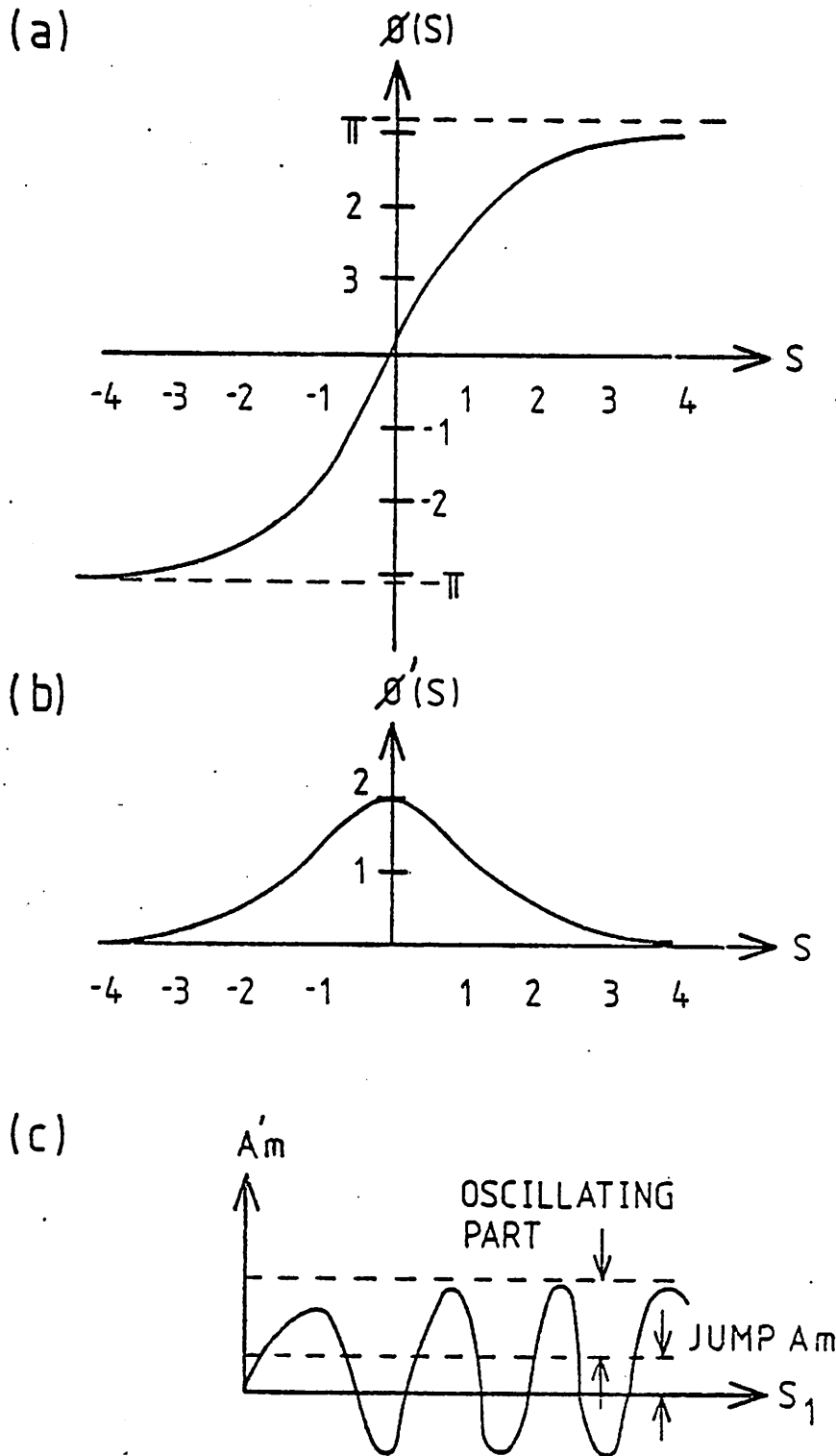


Fig.9 (a) The phase $\phi(s)$ and (b) the frequency $\phi'(s)$ for motion along the separatrix of a pendulum Hamiltonian; (c) the definition of $A'_m(s_1)$ showing the oscillating part, and the jump A_m , which is the Melnikov-Arnold integral.

where $\phi(s)$ is the separatrix phase motion, are actually improper; no limit exists. However, as shown in Fig.9c, they are the sum of a rapidly oscillating part and a "jump". The oscillating part may be large compared with the jump, but produces only a bounded oscillation in H_x which is not randomized on the timescale of the separatrix motion and averages to zero. The jump in (23) is known as the Melnikov-Arnold integral¹³, and physically gives the change in H_x due to resonance between harmonics of the separatrix motion of ϕ and the libration motion of θ .

Using (23) in (19),

$$\Delta H_x = \frac{1}{2} \mu \theta_0 r \sin(rs_0) \left[A_2(-r) - A_2(r) \right] \quad (24)$$

where

$$A_2(\pm r) = 4\pi r e^{\mp r/2} / \sinh(\pi r). \quad (25)$$

We have finally

$$\Delta H_x = 4\pi \mu \theta_0 r^2 \sin(rs_0) \sinh(\pi r/2) / \sinh(\pi r). \quad (26)$$

If we assume that $rs_0 = \chi_0$ is randomized after every half period of $\phi(n)$, then we can average ΔH_x^2 to get:

$$\langle \Delta H_x^2 \rangle_{s_0} = 8\pi^2 \mu^2 \theta_0^2 F(r) \quad (27)$$

where

$$F(r) = r^4 \sinh^2(\pi r/2) / \sinh^2(\pi r). \quad (28)$$

A plot of $F(r)$ is shown in Fig.10. It is sharply peaked close to $r=1$, suggesting that if the characteristic frequencies of the separatrix and libration motion differ by as much as a factor of four, the diffusion will be reduced by two orders of magnitude.

To obtain the diffusion coefficient, we need to know the mean half period of the motion in the thin stochastic layer \bar{T}_y . The half period of a true pendulum that follows a trajectory very close to the separatrix is approximately:

$$T_y = \frac{1}{\omega_y} \ln \left| \frac{32}{W} \right| \quad (29)$$

where

$$W \equiv \frac{H_y - H_s}{H_s} \ll 1$$

and $H_s = \omega_y^2/h$ is the separatrix energy. Chirikov⁴ has shown that the average half period inside the stochastic layer may be computed by simply integrating the half period over the energy interval of the layer. The result is:

$$\bar{T}_y = \frac{1}{\omega_y} \ln \left| \frac{32e}{W_0} \right| \quad (30)$$

where W_0 is the relative energy at the edge of the layer (it has approximately the same magnitude on both sides of the separatrix) and e is the natural base. Chirikov has also calculated the layer width W_0 using the so-called "whisker mapping". In our calculations, we have used actual measurements of W_0 taken from computer generated plots of the

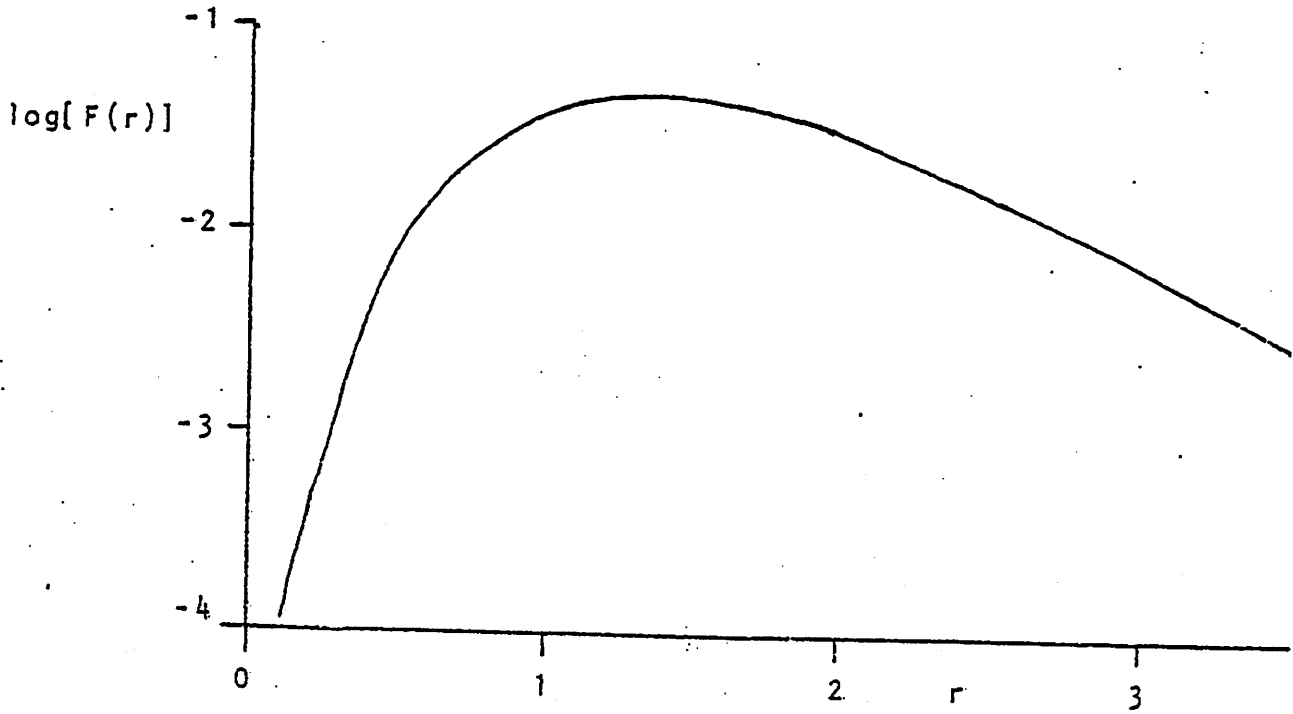


Fig.10. Plot of $F(r)$ for the dependence of thin layer diffusion on $r = \omega_x / \omega_y$.

uncoupled motion. The separatrix width is not appreciably affected by small couplings $\mu \ll a_y$.

Combining (27) and (30) we get the thin layer diffusion coefficient:

$$D_2 = \frac{\langle \Delta H_x^2 \rangle_{s_0}}{2T_y} \quad (31)$$

or

$$D_2 = 4\pi^2 \mu^2 \theta_0^2 \omega_y^2 F(r) / \ln(32e / |W_0|) \quad (32)$$

In Fig.11, the theoretical thin layer diffusion is compared with experimental measurements. Each triangle represents the final spread of 100 particles that have been started with identical initial conditions in the α -x space and slightly different initial conditions in the thin stochastic layer of the β -y space. The motion was followed for 2000 iterations and the RMS spread was computed using

$$\alpha_{\text{RMS}}^2 = \left(\frac{1}{100} \sum_{i=1}^{100} (\alpha^2 - \alpha_i^2) \right)^{\frac{1}{2}} \quad (33)$$

The theoretical curves were calculated from Eq.(32) with $W_0 = .191$. The variation of $(\alpha^2)_{\text{RMS}}$ with coupling strength is shown in Fig.11a. Variations with T_x and n are shown in Figs.11b and 11c, respectively. Again, the theoretical values fall slightly above the experimental, probably due to the fact that the y motion phase $\phi(n)$ is not completely

randomized with each successive half period of the separatrix motion. Phase correlations have been observed¹³ in a similar mapping for the Fermi problem. Nevertheless, theory and experiment agree surprisingly well, lending considerable support to the validity of the "stochastic pump" model of the Arnold diffusion.

VI COUPLING RESONANCE DIFFUSION

Returning now to the Hamiltonian (5), we investigate the Arnold diffusion in the vicinity of the coupling resonance $\omega_x = \omega_y$. For simplicity we choose $k_x = k_y = k$ and $a_x = a_y = a$ and consider the ordering $\mu \ll a \ll h$. The initial conditions have both α, x and β, y near their central resonances, yielding weakly nonlinear libration motion for both x and y . To proceed we transform (5) to explicitly exhibit the separatrix associated with the coupling resonance, and the resonances which drive the stochasticity across and along the separatrix layer. We first write $H = H_0 + \epsilon H_1$ where :

$$H_0 = h(\alpha^2 + \beta^2) - 2a(\cos kx + \cos ky) \quad (34)$$

and, keeping only quadratic terms in ϵH_1 and putting $\delta_1 \equiv 1$ in the coupling term:

$$\epsilon H_1 = -\mu k^2 xy - ak^2(1 - \delta_1)(x^2 + y^2). \quad (35)$$

$H_0 = H_{0x} + H_{0y}$ represents the sum of two identical, independent pendula. Transforming to action-angle variables

$J_x, J_y, \theta_x, \theta_y$ for these pendula, the new Hamiltonian has the form $H' = H'_0 + \epsilon H'_1$

where $H'_0 = G_0(J_x) + G_0(J_y)$ with

$$G_0(J) = \omega_0 J - \frac{1}{8} h k^2 J^2, \quad (36)$$

and with $\omega_0 = 2k(ah)^{\frac{1}{2}}$ the frequency for small amplitude librations. The frequency is:

$$\omega = d G_0 / dJ = \omega_0 - \frac{1}{4} h k^2 J \quad (37)$$

The perturbed Hamiltonian $\epsilon H'_1$ is given by (35) with x and y replaced by:

$$x = \sum_m b_m(J_x) \sin m\theta_x \quad (38)$$

$$y = \sum_m b_m(J_y) \sin m\theta_y,$$

where the sum is over odd integers. The first coefficient $b_1 = (2J/R)^{\frac{1}{2}}$, where $R = k(a/h)^{\frac{1}{2}}$, gives the transformation to action-angle variables for the harmonic oscillator. The remaining coefficients express the nonlinearity of the finite amplitude librations. The expansions in (36) and (38) can be obtained directly from the elliptic functions which give the pendulum motion, or from perturbation theory applied to a harmonic oscillator with a weak nonlinearity. Using (38) in (35) yields

$$\begin{aligned}
 \epsilon H'_1 = & - \mu k^2 \sum_{m,\ell} b_m(J_x) b_\ell(J_y) \sin m\theta_x \sin \ell\theta_y \\
 & - ak^2(1-\delta_1) \sum_{m,\ell} b_m(J_x) b_\ell(J_x) \sin m\theta_x \sin \ell\theta_x \\
 & - ak^2(1-\delta_1) \sum_{m,\ell} b_m(J_y) b_\ell(J_y) \sin m\theta_y \sin \ell\theta_y
 \end{aligned} \tag{39}$$

To exhibit the separatrix associated with the coupling resonance, we introduce sum and difference variables:

$$\begin{aligned}
 J_x &= \bar{J} + \tilde{J} & J_y &= \bar{J} - \tilde{J} \\
 \theta_x &= \frac{1}{2}(\bar{\theta} + \tilde{\theta}) & \theta_y &= \frac{1}{2}(\bar{\theta} - \tilde{\theta})
 \end{aligned} \tag{40}$$

and make the assumption that $\tilde{J} \ll \bar{J}$. Expanding H'_0 to second order in \tilde{J} yields the new zero order Hamiltonian K_0

$$K_0 = 2\omega_0 \bar{J} - \frac{1}{4} h k^2 (\bar{J}^2 + \tilde{J}^2) + \dots \tag{41}$$

In the perturbation $\epsilon H'_1$ we put $J_x = J_y = \bar{J}$ in the b's, use (7) for $\delta_1(n)$, and expand the sine and cosine products to obtain

$$\begin{aligned}
 \epsilon K_1 = & \frac{1}{2} \mu \sum_{\ell,m} \Lambda_{\ell m} \left[\cos(i\tilde{\theta} + j\bar{\theta}) - \cos(j\tilde{\theta} + i\bar{\theta}) \right] \\
 & + \frac{1}{2} a \sum_{\ell,m,q,\pm} \Lambda_{\ell m} \left[\cos(j\tilde{\theta} \pm j\bar{\theta} \pm 2\pi q n) - \cos(i\tilde{\theta} \pm i\bar{\theta} \pm 2\pi q n) \right],
 \end{aligned} \tag{42}$$

where $2i = \ell+m$, $2j = \ell-m$, $\Lambda_{\ell m} = k^2 b_\ell(\bar{J}) b_m(\bar{J})$, and the sums run over ℓ and m odd integers, q a positive (non-zero) integer, and all \pm terms indicated.

Equations (41) and (42) for the transformed Hamiltonian K are the starting point for application of the stochastic pump model to the coupling resonance, equivalent to the direct use of (5) for H in the analysis of thin layer diffusion. Writing $K = K'_0 + \epsilon K'_1$, we choose K'_0 to be the integrable part of K , consisting of K_0 and the first cosine term in the first sum in ϵK_1 , with $\ell=1$ and $m=1$:

$$K'_0 = 2\omega_0 \bar{J} - \frac{1}{4} h k^2 (\bar{J}^2 + \tilde{J}^2) + \frac{1}{2} \mu \Lambda_{11} \cos \tilde{\theta}. \quad (43)$$

The separatrix associated with the coupling resonance is apparent in (43). Assuming initial conditions on the separatrix, the unperturbed motion is $\bar{J} = \text{const}$, with

$$\theta = \bar{\omega} n + \bar{\theta}_0 \quad (45)$$

$$\tilde{\theta} = 4 \tan^{-1}(e^{\tilde{\omega} n}) - \pi \quad (46)$$

where $\bar{\omega} = 2\omega$, and $\tilde{\omega} = \frac{1}{2} k (h\mu\Lambda_{11})^{\frac{1}{2}}$ is the frequency of small amplitude librations in $\tilde{\theta}$.

To apply the stochastic pump model we must choose the two largest perturbation terms in $\epsilon K'_1$, with at least one term¹⁴ coming from the second sum in (42). For $\mu \ll \alpha$ and α -x and β -y libration motion not too near their central resonances, the two most important terms in $\epsilon K'_1$ both come

from the second sum in (42) with $q=1$.

$$\begin{aligned} \epsilon K_1' &= -\frac{1}{2} a \Lambda_1 \cos(i_1 \tilde{\theta} + i_1 \bar{\theta} - 2\pi n) \\ &\quad - \frac{1}{2} a \Lambda_2 \cos(i_2 \tilde{\theta} - i_2 \bar{\theta} + 2\pi n) \end{aligned} \quad (47)$$

where i_1 is the integer part of $2\pi/\bar{\omega}$, $i_2=i_1+1$, and Λ_1 and Λ_2 are the appropriate sums over the Λ_{lm} 's. Defining:

$$\delta\omega_1 = 2\pi - i_1 \bar{\omega} \quad (48)$$

$$\delta\omega_2 = i_2 \bar{\omega} - 2\pi \quad (49)$$

and assuming $\delta\omega_2 > \delta\omega_1$, we decompose the sum of (43) and (47) into $K = \bar{K} + \tilde{K}$, with the larger of the perturbation terms appearing in \tilde{K} :

$$\begin{aligned} \tilde{K} &= -\frac{1}{4} h k^2 J^2 + \frac{1}{2} \mu \Lambda_{11} \cos \tilde{\theta} \\ &\quad - \frac{1}{2} a \Lambda_1 \cos \left[i_1 \tilde{\theta} + i_1 \bar{\theta}(n) - 2\pi n \right] \end{aligned} \quad (47)$$

and

$$\bar{K} = \bar{\omega} \bar{J} - \frac{1}{2} a \Lambda_2 \cos \left[i_2 \tilde{\theta}(n) - i_2 \bar{\theta} + 2\pi n \right] \quad (48)$$

As before, we first solve (47) for $\tilde{\theta}$ and substitute this solution into (48). The Arnold diffusion is found from

$$\frac{d\bar{K}}{dn} = \frac{\partial \bar{K}}{\partial n} = \frac{1}{2} a \Lambda_2 (i_2 \frac{d\tilde{\theta}}{dn} + 2\pi) \sin(i_2 \tilde{\theta} - i_2 \bar{\theta} + 2\pi n). \quad (49)$$

After integration by parts and use of (49),

$$\begin{aligned} \frac{d\bar{K}}{dn} = & -\frac{1}{2} a \Lambda_2 \frac{d}{dn} \left[\cos(i_2 \tilde{\theta} - \delta \omega_2 n - i_2 \bar{\theta}_0) \right] \\ & + \frac{1}{2} a \Lambda_2 i_2 \frac{d\bar{\theta}}{dn} \sin(i_2 \tilde{\theta} - \delta_2 n - i_2 \bar{\theta}_0) \end{aligned} \quad (50)$$

The first term contributes only to a small oscillation with no net change in \bar{K} over long periods of time, and is ignored. Using (45) in (50),

$$\Delta \bar{K} = \frac{1}{2} a \Lambda_2 i_2 \bar{\omega} \int_{-\infty}^{\infty} \sin(i_2 \tilde{\theta} - \delta \omega_2 n - i_2 \bar{\theta}_0) dn \quad (51)$$

Putting $s = \tilde{\omega} n$, $r = \delta \omega_2 / \tilde{\omega}$, $s_0 = i_2 \bar{\theta}_0 / r$, $p = 2i_2$, $P = \bar{\omega} / \tilde{\omega}$ and taking the symmetric part of the integrand,

$$\Delta \bar{K} = -\frac{1}{2} a \Lambda_2 i_2 P \sin(s_0 r) A_p(r). \quad (52)$$

For $r \gg p$,

$$A_p(r) \sim \frac{4\pi(2r)^{p-1}}{(p-1)!} \exp\left(-\frac{\pi}{2}r\right) \quad (53)$$

The Arnold diffusion coefficient is:

$$D_3 = \frac{\langle \Delta \bar{K}^2 \rangle_{s_0}}{T_{\tilde{\theta}}} \quad (54)$$

where $T_{\tilde{\theta}}$ is the mean half-period in the separatrix layer, given by (30) with ω_y replaced by $\tilde{\omega}$.

The most important variation of D_3 is the variation with $r = \delta\omega_2/\bar{\omega}$. According to (48) and (49), $\delta\omega_2$ (defined to be always greater than or equal to $\delta\omega_1$) varies between $\bar{\omega}/2$ and $\bar{\omega}$, with the smallest $\delta\omega_2$ (largest diffusion rate) when $2\pi/\bar{\omega}$ is a half-integer, and the largest $\delta\omega_2$ (smallest rate) when $2\pi/\bar{\omega}$ is an integer. Since $\bar{\omega} = 4k\sqrt{ah}$ and $r \gg 1$, the diffusion rate varies over many orders of magnitude as k , a and h are varied to scan $\bar{\omega}$ over the half-integer to integer resonance with 2π , the fundamental driving (bounce) frequency. Choosing the half-integer resonance, we have:

$$r = \frac{\omega_0}{\omega} = \frac{4}{\theta_{ox}} \left(\frac{a}{\mu}\right)^{\frac{1}{2}} \quad (55)$$

where $\theta_{ox} = k x_{max}$ is the amplitude of the α -x libration oscillation. This variation of r yields a steep dependence of the diffusion rate on the oscillation amplitude and the coupling.

Before turning to a simpler example, we emphasize the remarkable character of the motion near this coupling resonance in the billiards system. For the initial conditions $\alpha=\beta=0$, $ky = -kx \ll 1$, the system is placed in the separatrix of the coupling resonance, and thus within the Arnold web. The billiard motion initially appears "to be stable", consisting of a fast bounce motion in z and slower, small amplitude oscillations in x and y ; in fact, it seems that the motion "is adiabatically confined" to a small neighbourhood near $x=y=0$. However, this is not the case. After a sufficient time, the billiard will be found, with very high

probability, in the "thick stochastic layer" for both its x and y motions. The manner in which the diffusion proceeds is illustrated in Fig.12, in the original angle-of-incidence (action) space of the system. A point (α, β) in this space is specified by the positive values of α "near" $x=0$ and β "near" $y=0$. The diffusion typically proceeds first along the coupling resonance, then along the thin layer in x or y , and finally along the corresponding thick layer. With very high probability, the billiard motion will rarely "become retrapped" in a concave ripple of the surface. This follows because the overwhelming fraction of the Arnold web is comprised of the "thick stochastic layers", with a negligible fraction of the web in regions, such as the coupling resonance, where the motion "appears to be adiabatic".

For the initial conditions $\alpha=\beta=0$, $k_y = k_x \ll 1$, the system is placed at the central fixed point of the coupling resonance. For these initial conditions, "not on the Arnold web", the motion is eternally confined to a small neighbourhood near $x=y=0$.

VII MANY RESONANCES

The previous calculations of the Arnold diffusion rate are analytically derived using only three resonances: The "guiding" resonance, along whose separatrix the diffusion takes place, and two "driving" resonances, the stronger driving the stochastic motion "across" the separatrix layer, the weaker driving the stochastic motion "along" the layer.

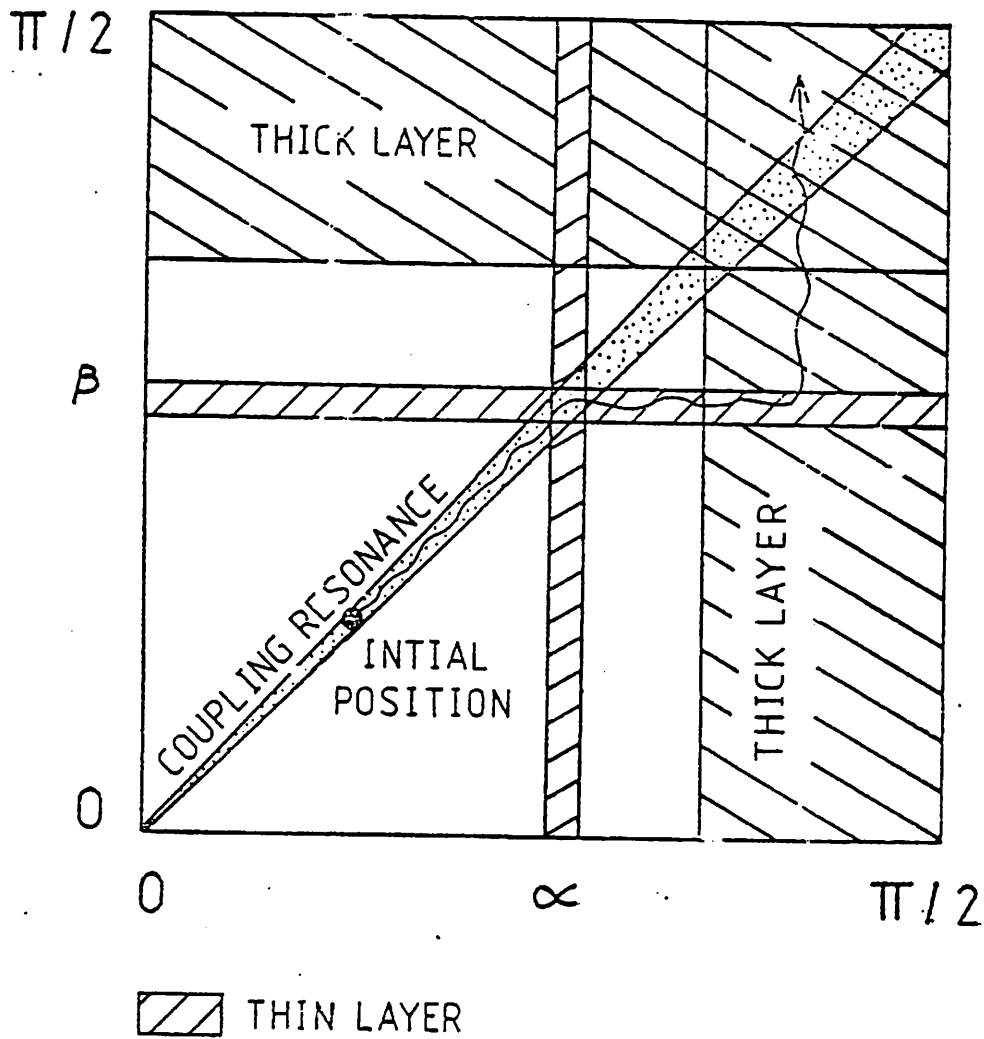


Fig.12 Arnold diffusion in the three dimensional billiards problem, in the angle of incidence space α - β . The initial condition is chosen to be within the separatrix of motion associated with the coupling resonance $\omega_x = \omega_y$. The initial motion with near normal incidence diffuses towards motion with large angles of incidence. A typical diffusive path is sketched.

These calculations seem to agree with numerical simulations provided the perturbation is not too weak. However, for sufficiently weak perturbations, many resonances are important, and the three wave theory predicts diffusion rates which are much lower than those calculated from numerical simulations. The many resonance regime is called the Nekhoroshev region^{7,9} after the Soviet mathematician who first derived a rigorous upper bound on the diffusion rate there. However, Nekhoroshev's upper bound is generally many orders of magnitude larger than the actual diffusion rate.

The many resonance regime has been examined numerically,^{4,9,11} and some analytic estimates made^{4,8,9} for a simpler model of a coupling resonance than that which we have considered for the billiards problem. The Hamiltonian studied was⁹:

$$H = \frac{1}{2}(p_1^2 + p_2^2) + \frac{1}{4}(x_1^4 + x_2^4) - \mu x_1 x_2 - \epsilon x_1 f(n) \quad (56)$$

where the p's are the momenta, the x's are the positions, and

$$f(n) = \frac{\cos \Omega n}{1 - A \cos \Omega n}$$
$$= \sum_m \frac{2e^{-\sigma m}}{\sigma} \cos m \Omega n \quad (57)$$

where $\sigma = (1 - A^2)^{\frac{1}{2}}$. This Hamiltonian differs from (34) and (35) in three major respects:

(1) The transformation to action-angle variables of H_0 is easily calculated. (2) The driving frequency Ω is chosen much less than the libration frequency ω for the p_1-x_1 and p_2-x_2 motions. (3) As a consequence of (2), the nonlinearity of the finite amplitude librations is negligible. In place of (38), we may use:

$$x_1 = b_1 \sin \theta_1 \quad (58)$$

The frequency difference $\delta\omega_2$, corresponding to (49) is:

$$\delta\omega_2 = 2\Omega - \omega \quad (59)$$

The minimum value of $\delta\omega_2$ is $\Omega/2$, giving a maximum diffusion coefficient of the form (54)

$$D \sim D_0 \exp(-\pi r) \quad (60)$$

where:

$$r = \delta\omega_2 / \tilde{\omega} \quad (61)$$

with $\tilde{\omega} \propto \mu^{1/2}$ the frequency for small amplitude librations within the coupling resonance as previously, and D_0 the non-exponential part of the coefficient, weakly dependent on the parameters. On the other hand, Nekhoroshev's best estimate for the upper bound on the diffusion rate is of the form:

$$D \sim D'_0 \exp(-\pi r^{1/Q}) \quad (62)$$

where for this system, Chirikov et al⁹ give Nekhoroshev's value as $Q = 4.5$.

Extensive numerical computations⁹ show that (60) is roughly correct for $r \lesssim 3$, with large deviations from this dependence for $r \gtrsim 3$. Figure 13 shows a plot of $\log D/D_0$ versus r taken from reference 9 which illustrates this point. The dashed line gives the prediction of the three resonance theory. The best fit to the numerical computations over the range $0.5 \lesssim r \lesssim 11$ seems to be for $Q=2$. This is illustrated in Fig.14, taken from reference 9, where the data of Fig.13 is replotted versus $r^{1/2}$. It is not known whether this result is generally applicable to all systems, or even whether it applies to diffusion along higher order resonances in the same system.

The enhancement in diffusion over that predicted by the three resonance theory arises from the nonlinearity in the finite amplitude librations, which were neglected in the calculation of (60). Indeed if we write in place of (58)

$$x_1 = \sum_m b_m \sin m \theta_1 \quad (63)$$

then

$$\delta\omega_2 = \ell\Omega - m\omega, \quad (64)$$

which shows that there are resonances with $r \rightarrow 0$, even though their harmonic amplitudes, which depend on the b 's, may be very small. It is these resonances which lead to the increased diffusion rate. A similar situation applies to the coupling resonance of the billiards problem, where the $q=1$ term was chosen in the expression (7) for $\delta_1(n)$. If all terms are kept, than (49) is replaced by:

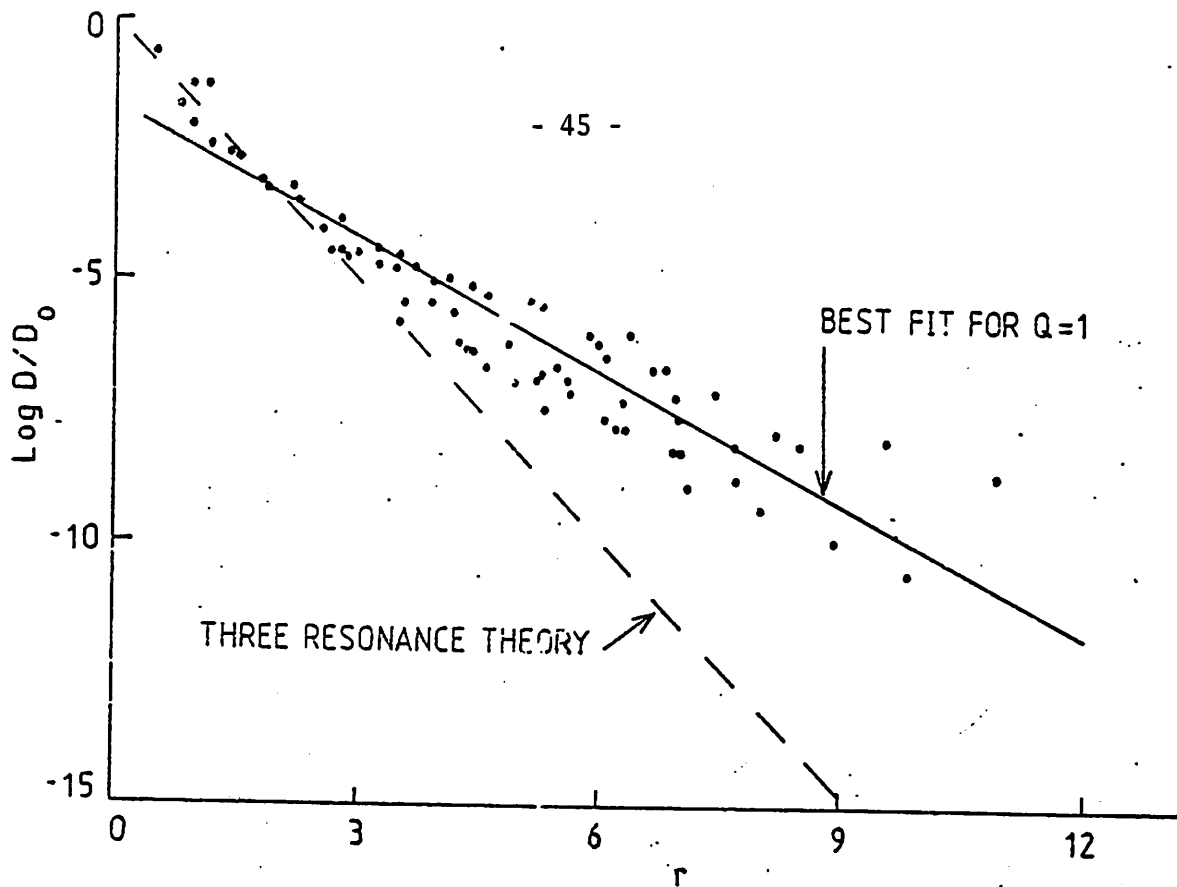


Fig.13 Arnold diffusion coefficient D versus $r = \delta\omega_2/\tilde{\omega}$ (after reference 9), showing the deviation from the three resonance theory (dashed line), and the best fit to the data points (solid line) for $Q=1$.

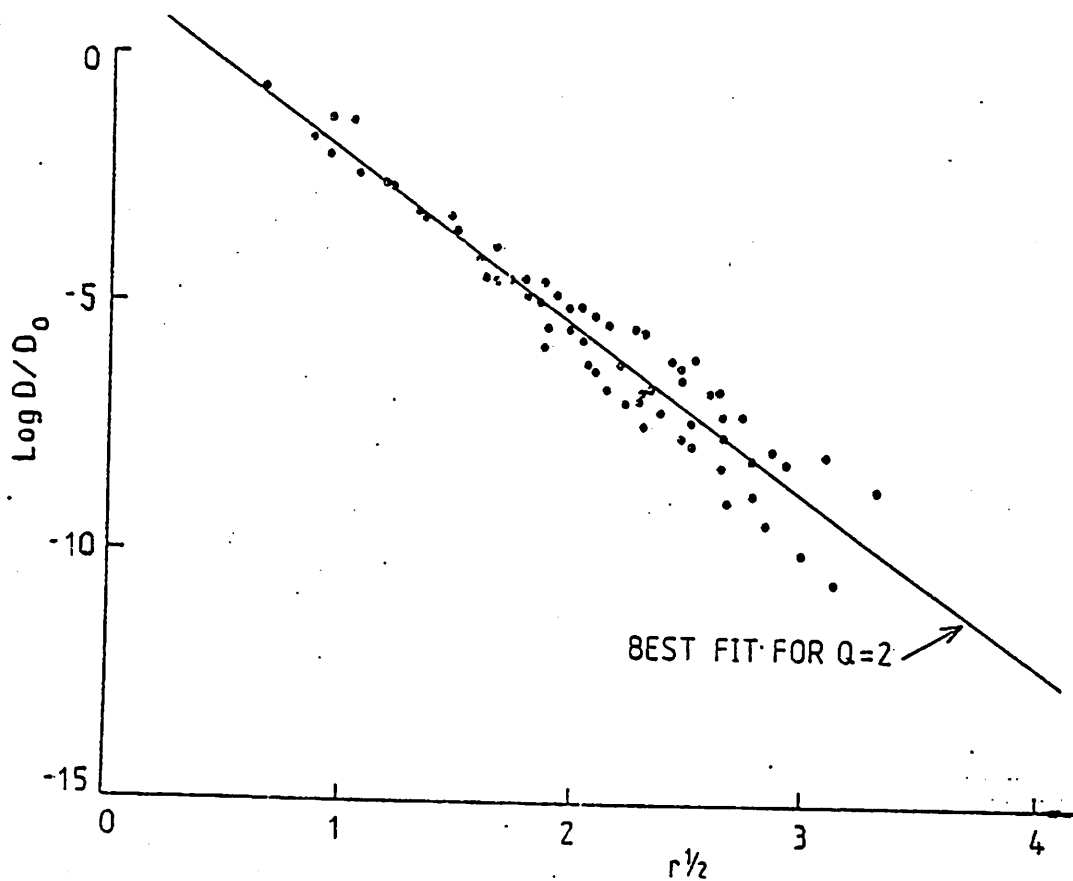


Fig.14 Arnold diffusion coefficient D versus $r^{1/2}$ (after reference 9) showing best fit to the data points

$$\delta\omega_2 = i_2\bar{\omega} - 2\pi q \quad (65)$$

again exhibiting the existence of resonances with $r \rightarrow 0$.
A theoretical method of calculating the diffusion rate in the Nekhoroshev regime has yet to grow "from alchemy into chemistry".

ACKNOWLEDGMENTS

I express my sincere appreciation to B. V. Chirikov, G. Contopolous, J. Ford, A. J. Lichtenberg and especially J. L. Tennyson for their interest, stimulating conversations and helpful comments. I thank B. V. Chirikov, J. Ford and F. Vivaldi for providing an advance copy of reference 9, M. G. Haines for the encouragement and physical facilities which enabled this work to be completed, and V. Collins for the preparation of the manuscript.

This work was supported by the Office of Naval Research Contract N00014-79-C-0674 and National Science Foundation Contract ENG 78-26372.

1. WHITTAKER, E.T. A Treatise on the Analytical Dynamics of Particles and Rigid Bodies, (Cambridge University Press, fourth edition, London 1937), p 313-314.
2. KOLMOGOROV, A.N. Dokl. Akad. Nauk SSSR 98 (1965) 527.
3. ARNOLD, V.I. and AVEZ, A. Ergodic Problems of Classical Mechanics (Benjamin, Inc., New York, 1968).
4. CHIRIKOV, B.V., "A Universal Instability of Many Dimensional Oscillator Systems", Phys.Reports 52, 5: 263-379 (1979).
5. ARNOLD, V.I. Dokl. Akad. Nauk SSSR 156, 9 (1964).
6. TENNYSON, J.L., M.A.LIEBERMAN and A.J. LICHTENBERG, "Diffusion in Near-Integrable Hamiltonian Systems with Three Degrees of Freedom", Symposium on Nonlinear Dynamics and the Beam-Beam Interaction, Conference Proceedings, American Institute of Physics, August 1979.
7. NEKHOROSHEV, N.N., Usp. Mat.Nauk USSR 32, 6 (1977).
8. CHIRIKOV, B.V., Fizika Plasmy 4, 3: 521 (1978).
9. CHIRIKOV, B.V., J.FORD and F. VIVALDI "Some Numerical Studies of Arnold Diffusion in a Simple Model", private communication, 1979.
10. FROESCHLE, C. Astrophys. Space Sci. 14, 110 (1971),
C. FROESCHLE and J.P. SCHEIDECKER, Astrophys. Space Sci. 25, 373 (1973).
11. GADIYAK, G.M., F.M. IZRAILEV, B.V. CHIRIKOV, Proc.7th Int'l Conf. on Nonlinear Oscillations (Berlin, 1975), vol.II, 1:315.

12. The assumption of a random phase for ϕ is not strictly correct. Near the edge of the thick layer, phase correlations are present due to KAM islands within the layer and other effects. A correction for this correlation can be made, but is not of great importance. See reference 4 for details.
13. MELNIKOV, V.K. Dokl Akad.Nauk SSSR 144, 747 (1962); 148, 1257 (1963); Trudy Moskovskova Mat. Obschestra 12, 3 (1963). See also ref. 4 (Appendix) and ref.5.
14. The three resonances must "form the basis" of the three degrees of freedom. It is easy to see that the problem becomes essentially two dimensional if all terms in the second sum of (42) are neglected. Motion along the separatrix layers is forbidden in this case.

FIGURE CAPTIONS

Fig.1 Isolation of regions by KAM surfaces (lines). In (a), the plane is divided by lines into a set of closed areas; in (b), the volume is not divided by lines into a set of closed volumes.

Fig.2 An illustration of Arnold diffusion. The resonance is at the origin, with the separatrix surrounding it. Stochastic motion across the layer, and the slow Arnold diffusion along the layer, are shown.

Fig.3 The three dimensional billiards problem. A point particle bounces back and forth between a smooth and a periodically rippled wall.

Fig.4 Motion in two degrees of freedom, illustrating the definition of the angle of incidence (action) α_n , and the bounce position x_n just before the n^{th} collision with the rippled wall.

Fig.5 Motion in the α - x surface of section for the uncoupled billiards problem. The parameters are $\mu=0$, with $\lambda_x:h:a_x$ as 100:10:2; $\lambda_x = 2\pi/k_x$. Fifteen particles are started at $x=0$ for various α 's and allowed to run for 1000 iterations each.

Fig.6 Thick layer diffusion for the coupled billiards problem. Initial conditions are close to the central resonance in the α - x space and within the thick stochastic layer (near $|\beta| = \pi/2$) of the β - y space. Parameters are $\mu/h = .008$ with $\lambda_x:h:a_x$ and $\lambda_y:h:a_y$ as 100:10:2.

Fig.7 Thick layer diffusion. Comparison of the theoretical diffusion with the results of simulation experiments. In (a), the dispersion is plotted vs the coupling amplitude μ . In (b) the dispersion is plotted vs the

libration period T_x . In (c), the dispersion vs the number of iterations n is shown. Parameters (except for those varied) are $\mu/h = .0002$; $n = 500$; $\lambda_x:h:a_x$ as 10:10:1; and $\lambda_y:h:a_y$ as 100:10:1.7. The statistical spread of the 100 particles is within the height of the triangles.

Fig.8 Thin layer diffusion. Initial conditions are close to the central resonance in the α - x space and within the separatrix stochastic layer in the β - y space. Parameters are the same as Fig.6. For convenience, both the α - x and β - y surface of sections are superimposed on the same figure.

Fig.9 (a) The phase $\phi(s)$ and (b) the frequency $\phi'(s)$ for motion along the separatrix of a pendulum Hamiltonian; (a) the definition of $A'_m(s_1)$ showing the oscillating part, and the jump A_m , which is the Melnikov-Arnold integral.

Fig.10 Plot of $F(r)$ for the dependence of thin layer diffusion on $r = \omega_x/\omega_y$.

Fig.11 Thin layer diffusion. Comparison of the theoretical diffusion with the results of simulation experiments. The three graphs show the variation with μ , T_x and n . Parameters (except for those varied) are $\mu/h = .0002$; $n = 2000$; $\lambda_x:h:a_x$ as 100:10:1; and $\lambda_y:h:a_y$ as 100:10:1.8. The statistical spread of the 100 particles is within the height of the triangles.

Fig.12 Arnold diffusion in the three dimensional billiards problem, in the angle of incidence space α - β . The initial condition is chosen to be within the

separatrix of motion associated with the coupling resonance $\omega_x = \omega_y$. The initial motion with near normal incidence diffuses towards motion with large angles of incidence. A typical diffusive path is sketched.

Fig.13 Arnold diffusion coefficient D versus $r = \delta\omega_2/\tilde{\omega}$ (after reference 9), showing the deviation from the three resonance theory (dashed line), and the best fit to the data points (solid line) for Q=1.

Fig.14 Arnold diffusion coefficient D versus $r^{1/2}$ (after reference 9), showing best fit to the data points (solid line) for Q=2.